(t, 1 H, H-5c), 3.63–3.59 (m, 2 H, H-3e, 6e), 3.53 (t, 1 H, H-6'e), 3.50–3.49 (m, 2 H, H-6f, 6'f), 3.47 (t, 1 H, H-3f), 3.44 (t, 1 H, H-4e), 3.39 (t, 1 H, H-2f), 3.36 (t, 1 H, H-2e), 3.14 (m, 1 H, H-5f), 2.22 (dd, 1 H, J_{gem}=13.7 Hz, $J_{3eq,4}$=4.8 Hz, H-3b$_{eq}$), 1.93 (t, 1 H, H-3b$_{ax}$), 2.19–1.75 (9 s, 27 H, 9 Ac); ^{13}C-NMR (100 MHz, $CDCl_3$) δ 170.7, 170.4, 170.3, 170.2, 169.7, 169.6, 168.0, 165.8, 164.1, 138.8, 138.6, 138.5, 138.4, 138.3, 137.9, 137.5, 133.2, 133.1, 129.9, 129.4, 128.4, 128.3, 128.3, 128.2, 128.2, 128.2, 128.1, 128.1, 128.0, 127.8, 127.8, 127.6, 127.5, 127.5, 127.3, 127.0, 103.7, 102.6, 101.1, 100.0, 98.6, 84.6, 82.6, 82.2, 81.6, 78.2, 77.1, 76.2, 76.2, 75.6, 75.1, 74.8, 74.7, 74.3, 73.9, 73.1, 72.0, 72.0, 71.2, 71.1, 70.3, 70.0, 68.9, 68.3, 68.2, 67.2, 67.1, 66.3, 63.3, 62.1, 61.4, 53.1, 51.5, 49.1, 35.8, 29.6, 23.2, 23.1, 21.0, 20.8, 20.7, 20.7, 20.5, 20.4, 20.3; MALDI MS: *m/z*: calcd for $C_{115}H_{128}N_2O_{38}Na$: 2,167.80; found: 2,167.91 $[M + Na]^+$.

Benzyl 2,3,4,6-tetra-O-acetyl-β-D-galactopyranosyl-(1→3)-2-acetamido-4,6-di-O-acetyl-2-deoxy-β-D-galactopyranosyl-(1→4)-{methyl 5-acetamido-4,7,8,9-tetra-O-acetyl-3,5-dideoxy-D-glycero-α-D-galacto-2-nonulopyranosylonate-(2→3)}-2,6-di-O-benzoyl-β-D-galactopyranosyl-(1→4)-2,3,6-tri-O-benzyl-β-D-glucopyranosyl-(1→6)-2,3,4-tri-O-benzyl-β-D-glucopyranoside (**24**) To a solution of compound **15** (105 mg, 64.5 μmol) and **21** (137 mg, 129 μmol) in CH_2Cl_2 (1.9 ml) was added molecular sieves 4 Å (300 mg). The suspension was stirred for 30 min and cooled to 0°C. To the mixture was added TMSOTf (1.2 μl, 6.5 μmol) and stirring was continued for 45 min. Completion of the reaction was confirmed by TLC (toluene/EtOAc=7:1). The reaction mixture was filtered through Celite. The combined filtrate and washings was extracted with $CHCl_3$, and the organic layer was washed with sat. Na_2CO_3 and brine, dried over Na_2SO_4 and concentrated. The residue was purified with column chromatography on silica gel ($CHCl_3$/MeOH=200:3) to give **24** (110 mg, 69%).; $[\alpha]_D$=+ 0.0° (*c* 0.8, $CHCl_3$); ^{1}H-NMR (600 MHz, $CDCl_3$): δ 8.18–7.09 (m, 45 H, 9 Ph), 5.88 (d, 1 H, $J_{5,NH}$=6.3 Hz, NH-c), 5.66 (m, 1 H, H-8b), 5.38–5.31 (m, 3 H, H-2a, 4c, 4d), 5.19 (dd, 1 H, $J_{6,7}$= 2.3 Hz, $J_{7,8}$=9.7 Hz, H-7b), 5.15 (d, 1 H, $J_{1,2}$=8.0 Hz, H-1c), 5.11–5.07 (m, 2 H, H-3a, 2d), 5.01–4.58 (m, 17 H, H-6a, 4b, 3c, 1d, 3d, 1f, NH-b, 10 CH*H*Ph), 4.48–4.37 (m, 5 H, $J_{1,2}$=7.4 Hz, H-1a, $J_{1,2}$=8.1 Hz, H-1e, 6e, 2 CH*H*Ph), 4.29–4.22 (m, 3 H, H-9b, 2 CH*H*Ph), 4.12–3.25 (m, 28 H, H-4a, 5a, 6a, 6'a, 5b, 6b, 9'b, 2c, 5c, 6c, 6'c, 5d, 6d, 6'd, 2e, 3e, 4e, 5e, 6'e, 2f, 3f, 4f, 5f, 6f, 6'f, -OMe), 2.73 (dd, 1 H, J_{gem}= 12.6 Hz, $J_{3eq,4}$=4.3 Hz, H-3b$_{eq}$), 2.19–1.49 (m, 37 H, H-3b$_{ax}$, 12 Ac); ^{13}C-NMR (150 MHz, $CDCl_3$) δ 172.1, 170.9, 170.7, 170.5, 170.3, 170.2, 170.2, 170.0, 169.3, 168.4, 165.5, 165.1, 138.9, 138.6, 138.6, 138.5, 138.1, 137.6, 133.4, 133.1, 130.3, 130.1, 130.0, 129.6, 128.7, 128.4, 128.2, 128.0, 128.0, 127.9, 127.8, 127.7, 127.7, 127.6, 127.3, 127.3, 103.8, 102.7, 101.1, 100.7, 99.0, 97.9, 84.7, 83.2, 82.4, 81.8, 78.3, 75.7, 75.2, 75.0, 75.0, 74.8, 74.5, 73.9, 73.6, 72.9, 72.2, 71.9, 71.6, 71.3, 71.0, 70.6, 69.2, 69.1, 69.0, 68.6, 67.1, 66.9, 66.6, 63.2, 62.8, 62.6, 61.0, 55.3, 52.8, 49.3, 36.9, 29.8, 24.0, 23.2, 22.8, 21.4, 20.9, 20.8, 20.8, 20.8, 20.7, 20.7, 20.4, 20.3, MALDI MS: *m/z*: calcd for $C_{127}H_{144}N_2O_{46}Na$: 2,455.89; found: 2,455.52 $[M + Na]^+$.

β-D-Galactopyranosyl-(1→3)-2-acetamido-2-deoxy-β-D-galactopyranosyl-(1→4)-{5-acetamido-3,5-dideoxy-D-glycero-α-D-galacto-2-nonulopyranosylonic acid-(2→3)}-β-D-galactopyranosyl-(1→4)-β-D-glucopyranosyl-(1→6)-β-D-glucopyranose (**1**) To a solution of compound **24** (95 mg, 39 μmol) in MeOH (1.6 ml) was added sodium methoxide (28% in MeOH; 14 mg). The mixture was stirred for 74 h under reflux condition, as the proceeding of the reaction was monitored by TLC ($CHCl_3$/MeOH/H_2O=3:2:0.3). H_2O (1.6 ml) was then added and stirring was continued for 14 h at ambient temperature. The reaction mixture was neutralized with Dowex (H^+) and filtered through cotton. The combined filtrate and washings was concentrated under diminished pressure to give a syrup compound. To a solution of the residue in H_2O (1.4 ml) was added palladium hydroxide [$Pd(OH)_2$] (20 wt% Pd on carbon; 345 mg). The mixture was vigorously stirred for 4 h at 40°C under hydrogen atmosphere, as the proceeding of the reaction was monitored by TLC (1-BuOH/MeOH/H_2O= 2:1:1). The reaction mixture was filtered through Celite, and the combined filtrate and washings was concentrated. The residue was purified with gel filtration column chromatography (Sephadex LH-20, H_2O as eluent) to give **1** (43 mg, 99%).; $[\alpha]_D$=+ 0.1° (*c* 1.0, H_2O); ^{1}H-NMR (600 MHz, CD_3OD): δ 5.16 (d, 1 H, $J_{1,2}$=3.7 Hz, H-1e), 4.79 (d, 1 H, H-1c), 4.57 (d, 1 H, $J_{1,2}$=8.0 Hz, H-1d), 4.49–4.45 (m, 3 H,H-1a, 1b, 1f), 4.15–3.19 (m, 39 H, ring H), 2.62 (dd, 1 H, H-3b$_{eq}$), 1.99 and 1.96 (2 s, 6 H, 2 Ac), 1.87 (m, 1 H, H-3b$_{ax}$), ^{13}C-NMR (150 MHz, CD_3OD) δ 175.0, 174.8, 174.1, 106.1, 105.7, 105.5, 104.1, 104.0, 103.4, 101.8, 97.0, 95.3, 94.2, 93.0, 91.5, 84.4, 81.2, 78.1, 77.6, 76.5, 75.1, 74.8, 74.5, 74.3, 73.9, 73.5, 73.4, 72.6, 72.1, 71.5, 70.8, 70.2, 68.9, 68.0, 67.1, 61.2, 61.0, 60.7, 59.7, 59.3, 58.8, 52.5, 51.6, 48.8, 47.5, 28.7, 25.9, 23.5; MALDI MS: *m/z*: calcd for $C_{43}H_{72}N_2O_{34}$: 1160.40; found: 1159.75 $[M\text{-}H]^-$.

2-Acetamido-2-deoxy-β-D-galactopyranosyl-(1→4)-{5-acetamido-3,5-dideoxy-D-glycero-α-D-galacto-2-nonulopyranosylonic acid-(2→3)}-β-D-galactopyranosyl-(1→4)-β-D-glucopyranosyl-(1→6)-D-glucopyranose (**2**) To a solution of compound **23** (38 mg, 18 μmol) in MeOH (2.0 ml) was added catalytic amounts of sodium methoxide (10 mg). The mixture was stirred for 96 h under reflux conditions, as

the proceeding of the reaction was monitored by TLC (1-BuOH/MeOH/H_2O=4:1:1). H_2O was then added and stirring was continued for 10 h at ambient temperature. The reaction mixture was neutralized with Dowex (H^+) and filtered through cotton. The combined filtrate and washings was concentrated under diminished pressure to give a syrupy compound. The residue was purified by gel filtration column chromatography on Sephadex LH-20 (MeOH) to give a white solid. To a solution of the solid in MeOH/H_2O (2.5/1 ml) was added palladium hydroxide [$Pd(OH)_2$] (20 wt% Pd on carbon; 40 mg). The mixture was vigorously stirred overnight at 40°C under hydrogen atmosphere, as the proceeding of the reaction was monitored by TLC (1-BuOH/MeOH/H_2O=2:1:1). The reaction mixture was filtered through Celite. The combined filtrate and washings was concentrated. The residue was purified with gel filtration column chromatography (Sephadex LH-20, MeOH/H_2O=1:1 as eluent) using MeOH as eluent, to give **2** (18 mg, 98%).; $[\alpha]_D$=+19.4° (*c* 1.7, MeOH:H_2O=1:1); ^{1}H-NMR (500 MHz, CD_3OD/D_2O=1:1): δ 2.69 (dd, 1 H, J_{gem}=11.4 Hz, $J_{3eq,4}$=4.6 Hz, H-3b_{eq}), 2.04 and 2.02 (2 s, 6 H, 2 NAc), 1.91 (t, 1 H, H-3b_{ax}); ^{13}C-NMR (125 MHz, CD_3OD/D_2O=1:1) δ 176.0, 175.4, 175.0, 103.9, 103.9, 103.7, 102.9, 97.3, 93.4, 80.0, 78.5, 77.0, 76.1, 75.8, 75.6, 75.4, 75.1, 71.0, 70.8, 69.8, 69.6, 69.5, 69.1, 64.2, 62.3, 61.5, 61.2, 53.5, 53.0, 49.5, 49.4, 48.4, 38.0, 23.6, 22.8; MALDI MS: *m/z*: calcd for $C_{37}H_{61}N_2O_{29}$: 997.33; found: 997.25 [*M*-H]$^-$.

{5-Acetamido-3,5-dideoxy-D-glycero-α-D-galacto-2-nonulopyranosylonic acid-(2→3)}-β-D-galactopyranosyl-(1→4)-β-D-glucopyranosyl-(1→6)-D-glucopyranose **(3)** To a solution of compound **22** (45 mg, 24 μmol) in MeOH (3.0 ml) was added sodium methoxide (28% in MeOH; 11 mg). The mixture was stirred for 48 h at 45°C, as the proceeding of the reaction was monitored by TLC ($CHCl_3$/MeOH=5:1). H_2O (1.0 ml) was then added and stirring was continued for 18 h at 45°C. The reaction mixture was neutralized with Dowex (H^+) and filtered through cotton. The combined filtrate and washings was concentrated under diminished pressure to give a syrupy compound. To a solution of the residue in H_2O (2.0 ml) was added palladium hydroxide [$Pd(OH)_2$] (20 wt% Pd on carbon; 100 mg). The mixture was stirred for 8 h at ambient temperature under hydrogen atmosphere, as the proceeding of the reaction was monitored by TLC ($CHCl_3$/MeOH/H_2O=3:1:0.1). The reaction mixture was filtered through Celite. The combined filtrate and washings was concentrated. The residue was purified with gel filtration column chromatography (Sephadex LH-20, H_2O as eluent) to give **3** (14 mg, 76%).: $[\alpha]_D$=+ 8.3° (*c* 0.6, H_2O); ^{1}H-NMR (400 MHz, D_2O): δ 5.21 (d, 1 H, $J_{1,2}$=3.7 Hz, H-1e), 4.64–4.51 (m, 2 H, H-1a, 1f), 4.21–2.87 (m, 25 H, ring H), 2.75 (dd, 1 H, J_{gem}=12.0 Hz, $J_{3eq,4}$=4.6 Hz, H-3b_{eq}), 2.02 (s, 3 H, Ac), 1.77 (m, 1 H, H-3b_{ax}), ^{13}C-NMR (100 MHz, D_2O) δ 177.7, 176.6, 105.4, 105.2, 102.5, 98.7, 94.8, 80.9, 78.4, 77.9, 77.6, 77.5, 77.5, 77.0, 76.7, 75.6, 75.5, 75.4, 74.5, 74.1, 73.1, 72.2, 72.1, 71.5, 71.4, 71.1, 70.8, 70.2, 65.3, 65.2, 63.7, 62.7, 57.1, 54.4, 42.4, 24.8, 21.8, 17.7; MALDI MS: *m/z*: calcd for $C_{29}H_{24}NO_{24}$: 795.26; found: 794.24 [*M*-H]$^-$.

Acknowledgements This work was financially supported by the Ministry of Education, Culture, Sports, Science, and Technology (MEXT) of Japan (Grant-in-Aid for Scientific Research to M. K., No. 17101007), the Ministry of Health, Labour and Welfare of Japan (Health and Labour Sciences Research Grants), and CREST of JST (Japan Science and Technology Agency).

References

1. Allende, M.L., Proia, R.L.: Lubricating cell signaling pathways with gangliosides. Curr. Opin. Struct. Biol. **12**, 587–592 (2002)
2. Crocker, P.R., Paulson, J.C., Varki, A.: Siglecs and their roles in the immune system. Nat. Rev. Immunol. **7**, 255–266 (2007)
3. Holmgren, J., Lönnroth, I., Svennerholm, L.: Tissue receptor for cholera exotoxin: Postulated structure from studies with GM1 ganglioside and related glycolipids. Infect. Immunity **8**, 208–214 (1973)
4. Jolivet-Reynaud, C., Hauttecoeur, B., Alouf, J.E.: Interaction of *Clostridium perfringens* delta toxin with erythrocyte and liposome membranes and relation with the specific binding to the ganglioside GM2. Toxicon **27**, 1113–1126 (1989)
5. Fuster, M.M., Esko, J.D.: The sweet and sour of cancer: glycans as novel therapeutic targets. Nat. Rev. Cancer **5**, 526–542 (2005)
6. Jeyakumar, M., Dwek, R.A., Butters, T.D., Platt, F.M.: Storage solutions: treating lysosomal disorders of the brain. Nat. Rev. Neurosci. **6**, 1–12 (2005)
7. Feizi, T., Fazio, F., Chai, W., Wong, C.-H.: Carbohydrate microarrays: a new set of technologies at the frontiers of glycomics. Curr. Opin. Struct. Biol. **13**, 637–645 (2003) and references therein)
8. Fazio, F., Bryan, M.C., Blixt, O., Paulson, J.C., Wong, C.-H.: Synthesis of sugar arrays in microtiter plate. J. Am. Chem. Soc. **124**, 14397–14402 (2002)
9. Adams, E.W., Daniel, M.R., Bokesch, H.R., McMahon, J.B., O'Keefe, B.R., Seeberger, P.H.: Oligosaccharide and glycoprotein microarrays as tools in HIV glycobiology: Glycan–dependent gp120/protein interactions. Chem. Biol. **11**, 875–881 (2004)
10. Park, S., Shin, I.: Fabrication of carbohydrate chips for studying protein–carbohydrate interactions. Angew. Chem. Int. Ed. Engl. **41**, 3180–3182 (2002)
11. Suda, Y., Arano, A., Fukui, Y., Koshida, S., Wakao, M., Nishimura, T., Kusumoto, S., Sobel, M.: Immobilization and clustering of structurally defined oligosaccharides for sugar chips: An improved method for surface plasmon resonance analysis of protein–carbohydrate interactions. Bioconjugate Chem. **17**, 1125–1135 (2006)
12. Wang, D., Liu, S., Trummer, B.J., Deng, C., Wang, A.: Carbohydrate microarrays for the recognition of cross-reactive molecular markers of microbes and host cells. Nat. Biotechnol. **20**, 275–281 (2002)

13. Willats, W.G., Rasmussen, S.E., Kristensen, T., Mikkelsen, J.D., Knox, J.P.: Sugar-coated microarrays: A novel slide surface for the high-throughput analysis of glycans. Proteomics **2**,1666–1671 (2002)
14. Fuse, T., Ando, H., Imamura, A., Sawada, N., Ishida, H., Kiso, M., Ando, T., Li, S.-C., Li, Y.-T.: Synthesis and enzymatic susceptibility of a series of novel GM2 analogs. Glycoconjugate J. **23**, 329–343 (2006)
15. Ando, H., Koike, Y., Ishida, H., Kiso, M.: Extending the possibility of an *N*-Troc-protected sialic acid donor toward variant sialo-glycoside synthesis. Tetrahedron Lett. **44**, 6883–6886 (2003)
16. Ando, H., Imamura, A.: Proceedings in synthetic chemistry of sialo-glycoside. Trend. Glycosci. Glycotech. **16**, 293–303 (2004)
17. Yoshikawa, T., Kato, Y., Yuki, N., Yabe, T., Ishida, H., Kiso, M.: A highly efficient construction of GM1 epitope tetrasaccharide and its conjugation with KLH. Glycoconjugate J. (2008) (in press)
18. Veeneman, G.H., van Leeuwen, S.H., van Boom, J.H.: Iodonium ion promoted reactions at the anomeric centre. II An efficient thioglycoside mediated approach toward the formation of 1,2-*trans* linked glycosides and glycosidic esters. Tetrahedron Lett. **31**, 1331–1334 (1990)
19. Cook, A.F.: Use of 2,2,2-tribromoethyl chloroformate for the protection of nucleoside hydroxyl groups. J. Org. Chem **33**, 3589–3593 (1968)
20. Burke, S.D., Danheiser, R.L. (eds). Handbook of Reagents for Organic Synthesis, Oxidizing and Reducing Agents, pp. 513–518. Wiley, Chichester (1999)
21. Matsuzaki, Y., Ito, Y., Nakahara, Y., Ogawa, T.: Synthesis of branched poly-*N*-acetyl-lactosamine type pentaantennary pentacosasaccharide: Glycan part of a glycosyl ceramide from rabbit erythrocyte membrane. Tetrahedron Lett. **34**, 1061–1064 (1993)
22. Pedretti, V., Mallet, J.-M., Sinaÿ, P.: Silylmethylene radical cyclization. A stereoselective approach to branched sugars. Carbohydr. Res. **244**, 247–257 (1993)
23. Lu, W., Navidpour, L., Taylor, S.D.: An expedient synthesis of benzyl 2,3,4-tri-*O*-benzyl-β-D-glucopyranoside and benzyl 2,3,4-tri-*O*-benzyl-β-D-mannopyranoside. Carbohydr. Res. **340**, 1213–1217 (2005)
24. Debenham, S.D., Toone, E.J.: Regioselective reduction of 4,6-*O*-benzylidenes using triethylsilane and BF_3-Et_2O. Tetrahedron: Asymmetry **11**, 385–387 (2000)

JOURNAL OF VIROLOGY, Apr. 2008, p. 3843–3852
0022-538X/08/$08.00+0 doi:10.1128/JVI.02013-07

Vol. 82, No. 8

Highly Enhanced Expression of CD70 on Human T-Lymphotropic Virus Type 1-Carrying T-Cell Lines and Adult T-Cell Leukemia Cells[▽]

Masanori Baba,[1]†* Mika Okamoto,[1]† Takayuki Hamasaki,[1] Sawako Horai,[2] Xin Wang,[1]‡ Yuji Ito,[3] Yasuo Suda,[4] and Naomichi Arima[2]

Division of Antiviral Chemotherapy, Center for Chronic Viral Diseases, Graduate School of Medical and Dental Sciences, Kagoshima University, Kagoshima 890-8544, Japan[1]; Division of Host Response, Center for Chronic Viral Diseases, Graduate School of Medical and Dental Sciences, Kagoshima University, Kagoshima 890-8544, Japan[2]; Department of Bioengineering, Faculty of Engineering, Kagoshima University, Kagoshima 890-0065, Japan[3]; and Nanostructured and Advanced Materials Course, Graduate School of Science and Engineering, Kagoshima University, Kagoshima 890-0065, Japan[4]

Received 11 September 2007/Accepted 30 January 2008

Human T-lymphotropic virus type 1 (HTLV-1) is the etiologic agent of adult T-cell leukemia (ATL). In Japan, the number of HTLV-1 carriers is estimated to be 1.2 million and more than 700 cases of ATL have been diagnosed every year. Considering the poor prognosis and lack of curative therapy of ATL, it seems mandatory to establish an effective strategy for the treatment of ATL. In this study, we attempted to identify the cell surface molecules that will become suitable targets of antibodies for anti-ATL therapy. The expression levels of approximately 40,000 host genes of three human T-cell lines carrying HTLV-1 genomes were analyzed by oligonucleotide microarray and compared with the expression levels of the genes in an HTLV-1-negative T-cell line. The HTLV-1-carrying T-cell lines used for experiments had totally different expression patterns of viral genome. Among the genes evaluated, the expression levels of 108 genes were found to be enhanced more than 10-fold in all of the T-cell lines examined and 11 of the 108 genes were considered to generate the proteins expressed on the cell surface. In particular, the CD70 gene was upregulated more than 1,000-fold and the enhanced expression of the CD70 molecule was confirmed by laser flow cytometry for various HTLV-1-carrying T-cell lines and primary CD4$^+$ T cells isolated from acute-type ATL patients. Such expression was not observed for primary CD4$^+$ T cells isolated from healthy donors. Since CD70 expression is strictly restricted in normal tissues, such as highly activated T and B cells, CD70 appears to be a potential target for effective antibody therapy against ATL.

Human T-lymphotropic virus type 1 (HTLV-1) is the etiologic agent of adult T-cell leukemia (ATL) and HTLV-1-associated myelopathy/tropical spastic paraparesis (10, 29, 40). The geographic distribution of the virus has been well defined, and the areas in the world where it is highly prevalent include Japan, Africa, the Caribbean islands, and South America (31). In Japan, the number of HTLV-1 carriers is estimated to be 1.2 million and more than 700 cases of ATL are diagnosed every year (37). Since conventional anticancer chemotherapy active against other lymphoid malignancies proved to be ineffective for treating aggressive types of ATL, combination chemotherapy designed exclusively for ATL has been examined. Although such chemotherapy considerably improved the treatment response rates in ATL patients, it could not sufficiently extend the median survival time (16, 39). Therefore, it seems still mandatory to establish an effective strategy for the treatment of ATL.

Monoclonal antibodies (MAbs) have recently gained considerable importance in the area of anticancer therapy. The first agent approved for clinical use is rituximab, which is an anti-CD20 mouse/human chimeric MAb (32). Rituximab was found to be effective for a variety of B-cell lymphomas as well as non-Hodgkin's lymphoma (12). Currently, several MAbs have been approved by the U.S. Food and Drug Administration for the treatment of lymphoma, leukemia, breast cancer, and metastatic colon cancer. One of the anticancer mechanisms of these MAbs is the induction of antibody-dependent cytotoxicity (15, 20). The antibodies bind to the surface antigens of tumor cells, while their crystallizable fragments (Fc) bind to the Fc receptors of the effector cells, such as natural killer cells and monocytes, triggering cytolysis of the target cells. In addition, complement-dependent cytotoxicity and direct induction of apoptosis are also considered anticancer mechanisms of the MAbs (20, 21).

A rationale of using MAbs for anticancer therapy is their high specificities to tumor cells. A certain number of antigens overexpressed on tumor cells have been identified as the targets of MAbs. Such antigens do not need to be completely absent from normal tissues, because their relative overexpression on tumor cells has proved to be sufficient to confer a high

* Corresponding author. Mailing address: Division of Antiviral Chemotherapy, Center for Chronic Viral Diseases, Graduate School of Medical and Dental Sciences, Kagoshima University, 8-35-1, Sakuragaoka, Kagoshima 890-8544, Japan. Phone: 81-99-275-5930. Fax: 81-99-275-5932. E-mail: m-baba@vanilla.ocn.ne.jp.

† These authors contributed equally to this work.

‡ Present address: Department of Pharmacology, Yale University School of Medicine, New Haven, CT 06520.

▽ Published ahead of print on 6 February 2008.

level of specificity of MAbs to the target cells (20). Nevertheless, MAbs with higher specificities would be preferable in terms of safety in vivo. Oligonucleotide microarray is an efficient tool for studying the comprehensive gene expression levels of tumor cells in comparison with normal tissues. In fact, several molecules overexpressed in ATL cells have been identified by this technology (7, 35). In these studies, clinical samples obtained from ATL patients were analyzed for their gene expression and compared with normal T cells. The advantage of this procedure is that the gene expression profiles of ATL cells in different disease types or stages can be analyzed directly. On the other hand, the expression profiles may be affected by several conditions of patients, such as the time of sample collection, the use of anticancer agents and/or other drugs, and the presence of complications. Therefore, the microarray analysis of primary ATL cells is not always an ideal way to identify the molecules commonly overexpressed in ATL cells.

The purpose of this study is to identify the surface molecules that will become potential targets for anti-ATL MAb therapy. To this end, the expression levels of approximately 40,000 host genes of three T-cell lines carrying HTLV-1 were analyzed by oligonucleotide microarray and compared with the levels in an HTLV-1-negative T-cell line. Among the genes that could be evaluated, the expressions of 108 genes were found to be enhanced more than 10-fold in all of the T-cell lines examined and 11 of the 108 genes were considered to generate the proteins expressed on the cell surface. In particular, the CD70 gene was upregulated tremendously (more than 1,000-fold), which was confirmed by the analysis for CD70 expression on various HTLV-1-carrying T-cell lines and primary $CD4^+$ T cells from ATL patients.

MATERIALS AND METHODS

Cells. The HTLV-1-carrying T-cell line S1T was established from the peripheral blood mononuclear cells (PBMCs) of an ATL patient, as described previously (2). The HTLV-1-carrying T-cell lines MT-2, MT-4, and M8166; the HTLV-1-negative T-cell lines MOLT-4, CEM, and Jurkat; and the monocytic cell lines HL-60 and U937 were also used for experiments. MT-2 and MT-4 cells are derived from umbilical cord blood lymphocytes after cocultivation with leukemia cells from ATL patients (24). MT-2 cells were reported to integrate at least eight copies, including defective types, of HTLV-1 proviral DNA in the chromosomes (18). M8166 is a subclone of C8166 cells, which were also established by cocultivation of umbilical cord blood lymphocytes with ATL cells. M8166 cells integrate one copy of provirus in the chromosome (34). All cell lines were maintained in RPMI 1640 medium supplemented with 10% heat-inactivated fetal bovine serum, 100 U/ml penicillin G, and 100 μg/ml streptomycin. PBMCs were donated under informed consent from patients with acute-type ATL and healthy volunteers. The cells were isolated from heparinized blood with Ficoll-Paque Plus (Pharmacia, Uppsala, Sweden) to obtain PBMCs. Diagnoses of ATL were based on clinical features, hematological characterization, the presence of serum antibodies against HTLV-1, and the insertion of proviral DNA into leukemia cells.

Characterization of HTLV-1-carrying T-cell lines. The production of viral antigens from S1T, MT-2, and M8166 cells into culture supernatants was determined by enzyme-linked immunosorbent assay (ELISA). Briefly, the cells (1×10^5 cells/ml) were incubated for 3 days at 37°C. After incubation, the culture supernatants were collected and examined for their p19 antigen levels with a sandwich enzyme-linked immunosorbent assay kit (Cellular Products, Buffalo, NY). The cells were also examined for their expression of HTLV-1 *env* and *tax* genes by reverse transcription-PCR (RT-PCR). For RT-PCR, the cells were harvested after a 3-day incubation and washed three times with ice-cold phosphate-buffered saline. Total RNA was extracted from the cells with an extraction kit (RNeasy; Qiagen, Hilden, Germany). The extracted RNA was treated with DNase I and subjected to RT-PCR. The primers used for RT-PCR were RENV1 (5′-ACGCCGGTTGAGTCGCGTTCT-3′), RENV4 (5′-CACCGAAGATGAG GGGGCAGA-3′), RPX3 (5′-ATCCCGTGGAGACTCCTCAA-3′), and RPX4 (5′-AACACGTAGACTGGGTATCC-3′). Glyceraldehyde-3-phosphate dehydrogenase (GAPDH) mRNA was also amplified as an internal control by the primer pair RT-GAPDH5 (5′-CATTGACCTCAACTACATGG-3′) and RT-GAPDH3 (5′-AGTGATGGCATGGACTGTGG-3′). The samples were subjected to reverse transcription to cDNA for 30 min at 42°C and PCR amplification (95°C for 30 s, 55°C for 30 s, and 72°C for 1 min) with each primer pair. The amplified products were analyzed by the 2100 Bioanalyzer (Agilent, Santa Clara, CA).

For the detection of HTLV-1 Tax, Western blot analysis of the cells was performed as described previously (41). Briefly, the cells were incubated for 3 days and lysates were obtained by treating the cells with a low-salt extraction buffer (10 mM Tris-HCl [pH 8.0] containing 0.14 M NaCl, 3 mM $MgCl_2$, 1 mM dithiothreitol, 2 mM phenylmethylsulfonyl fluoride, and 0.5% Nonidet P-40) on ice for 20 min. The lysates were centrifuged at $12,000 \times g$ at 4°C for 10 min. After measuring protein concentrations, the lysates (100 μg of protein) were electrophoresed on a 10% polyacrylamide gel with sodium dodecyl sulfate and transferred to a polyvinylidene difluoride membrane. The transferred proteins were reacted with the anti-p40 Tax MAb Lt-4 (38) or an anti-actin polyclonal antibody (Santa Cruz Biotechnology, Santa Cruz, CA), followed by treatment with horseradish peroxidase-conjugated goat anti-mouse immunoglobulin G (IgG) (Amersham Biosciences, Buckinghamshire, United Kingdom) or horseradish peroxidase-conjugated rabbit anti-goat IgG (MP Biomedicals, Solon, OH). Antibody binding was visualized with an enhanced chemiluminescence detection system (Amersham Biosciences).

Oligonucleotide microarray. S1T, M8166, MT-2, and MOLT-4 cells (1×10^5 cells/ml) were incubated for 3 days at 37°C. After incubation, total RNA was extracted from the cells with RNeasy (Qiagen). The quality of the total RNA was examined by the 2100 Bioanalyzer (Agilent), according to the manufacturer's protocol. The microarray processing of the samples was carried out with necessary reagent kits provided by Agilent, according to the manufacturer's one-color microarray-based gene expression analysis protocol (version 5.5). Briefly, 500 ng of the total RNA was reverse transcribed to cDNA with Moloney murine leukemia virus reverse transcriptase and T7 promoter primer. The cDNA was transcribed and amplified with T7 RNA polymerase to produce the cRNA labeled with cyanine 3. The cyanine 3-labeled cRNA was purified with RNeasy (Qiagen) and examined for its concentration and labeling quality by a spectrophotometer. The cRNA was fragmented and hybridized to Agilent whole human genome oligonucleotide microarray (4×44K slide format). After hybridization, the microarray was washed thoroughly and scanned with a microarray scanner (Agilent). The microarray scan data were processed with Future Extraction software (version 9.5.1; Agilent), according to its manual. Cell culture and microarray experiments were conducted simultaneously for all of the T-cell lines and repeated three times.

Data analysis. The expression level of each gene was analyzed by GeneSpring GX software (version 7.3.1; Agilent). Briefly, after importing the processed data into the software, they were normalized based on the default normalizing settings for one-color experiments (GeneSpring 7.3 user's guide; Agilent). The normalized data were filtered on the basis of parameters in certain specific columns of the original data files to remove the control and other inappropriate spots. The genes of which expression levels were more than 10-fold in all of the three HTLV-1-carrying T-cell lines (S1T, M8166, and MT-2) compared with the levels of the control T-cell line (MOLT-4) were selected and evaluated for their statistical significance by t test ($P < 0.05$) with multiple testing correction.

Flow cytometric analysis. The MAbs used for experiments were phycoerythrin (PE)-conjugated anti-human CD70 mouse MAbs (BD Biosciences, San Jose, CA [for staining cell lines] and BD Pharmingen, San Diego, CA [for staining PBMCs]), PE-conjugated anti-human CD124 mouse MAb (BD Biosciences), PE-conjugated anti-human interleukin-21 receptor (IL-21R) mouse MAb (R&D Systems, Minneapolis, MN), PE-conjugated anti-human CD151 mouse MAb (BD Biosciences), peridinin chlorophyll protein (PerCP)-conjugated anti-human CD3 mouse MAb (BD Biosciences), PerCP-conjugated anti-human CD4 mouse MAb (BD Biosciences), fluorescent isothiocyanate (FITC)-conjugated anti-human CD25 mouse MAb (Beckman Coulter, Fullerton, CA), FITC-conjugated anti-human CD8 mouse MAb (Beckman Coulter), PerCP-Cy5.5-conjugated anti-human CD19 mouse MAb (BD Biosciences), FITC-conjugated anti-human CD14 mouse MAb (BD Pharmingen), and their isotype-matched control MAbs. The test cell lines and PBMCs were washed with phosphate-buffered saline containing 1% bovine serum albumin and incubated with appropriate MAbs for 30 min at 4°C. After washing, the stained cells were analyzed by FACScan (Becton Dickinson, San Jose, CA).

Anti-cell proliferation assay. S1T and MOLT-4 cells were incubated (1×10^4 cells/well) in a flat-bottomed microtiter plate with an anti-human CD70 mouse MAb (BD Biosciences) or its isotype-matched control MAb at a concentration of 1 μg/ml. After incubation at 37°C, the number of viable cells was determined every day by trypan blue exclusion. For primary ATL cells, PBMCs were obtained from three different ATL patients and the cells (1×10^5 cells/well) were cultured in a microtiter plate with an anti-human CD70 mouse MAb (BD Pharmingen) or its isotype-matched control MAb at various concentrations. After a 24-h incubation, 25 μl of 3-(4,5-dimethylthiazol-2-yl)-2,5-diphenyltetrazolium bromide (MTT) (1 mg/ml) was added and further incubated at 37°C for 4 h. After incubation, 20% sodium dodecyl sulfate solution was added to each well. The plate was incubated overnight at room temperature in a dark place, and specific absorbance was read at 570 nm by a microplate reader.

RESULTS

Viral gene and antigen expression in HTLV-1-carrying T-cell lines. To identify the molecules selectively expressed in ATL cells, comprehensive gene expression in HTLV-1-carrying T-cell lines was examined by oligonucleotide microarray and compared with the gene expression in an HTLV-1-negative T-cell line. To this end, cell lines with various viral gene expression and replication patterns should be selected. Among the HTLV-1-carrying T-cell lines available in our laboratory, three T-cell lines, S1T, MT-2, and M8166, were selected and examined for their HTLV-1 gene expression, protein synthesis, and release of viral antigens in culture supernatants. The HTLV-1-negative T-cell leukemia line MOLT-4 was selected as a control. As shown in Fig. 1A, a strong signal of *tax* mRNA could be found in MT-2 and M8166 cells, whereas a significant signal of *env* mRNA was detected in only MT-2 cells. Like MOLT-4 cells, neither *env* nor *tax* mRNA was identified in S1T cells. These observations were confirmed by Western blot analysis of these cell lines, where sufficient amounts of p68 Env-Tax fusion protein and Tax were observed in MT-2 and M8166 cells, respectively (Fig. 1B). However, neither Tax nor Env could be detected in S1T cells. Furthermore, MT-2 cells produced and released a large amount of HTLV-1 p19 antigen, which is regarded as a component of viral particles, into culture supernatants, yet p19 production was not observed in M8166 and S1T cells (Fig. 1C). These results suggest that the three HTLV-1-carrying cell lines, of which viral gene expression patterns differ completely, are suitable tools for searching the host cellular genes and proteins commonly overexpressed in ATL cells obtained from patients.

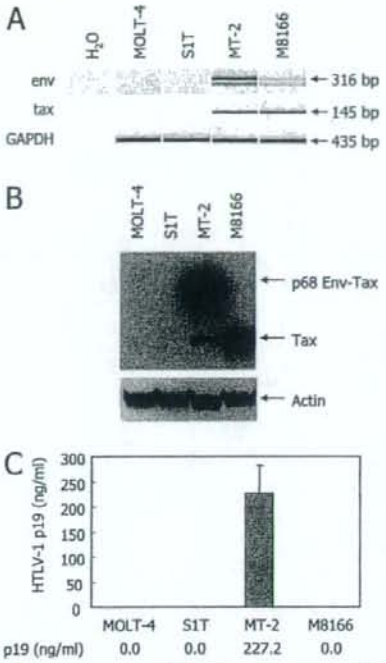

FIG. 1. Different patterns of viral gene expression in HTLV-1-carrying T-cell lines. (A) Detection of HTLV-1 *env* and *tax* gene expression in MOLT-4 (negative control), S1T, MT-2, and M1866 cells. Total RNA was extracted from the cells and subjected to RT-PCR with primer pairs described in Materials and Methods. GAPDH mRNA was also amplified as an internal control. The amplified products were analyzed by an Agilent Bioanalyzer. (B) Western blot analysis of the cells for detection of HTLV-1 Tax. The cell lysates were electrophoresed and transferred to a membrane, as described in Materials and Methods. The transferred proteins were reacted with an anti-p40 Tax MAb or an anti-actin polyclonal antibody, followed by treatment with the second antibody. Antibody binding was visualized with an enhanced chemiluminescence detection system. (C) The production of viral particles and antigens from the cells. The cells were incubated for 3 days. After incubation, culture supernatants were collected and examined for their p19 antigen levels by ELISA. The error bar indicates standard deviation.

Gene expression profiles in HTLV-1-carrying T-cell lines. The gene expression in the HTLV-1-carrying T-cell lines S1T, MT-2, and M8166 was examined and compared with the expression in the HTLV-1-negative T-cell line MOLT-4 by Agilent whole human genome oligonucleotide microarray (4 × 44K slide format). Among all the (41,150) genes that could be analyzed, the expression levels of 3,931 genes were modulated in all of the HTLV-1-carrying T-cell lines with statistical significance ($P < 0.05$) (data not shown). Furthermore, among the 3,931 genes, 108 genes were upregulated more than 10-fold, respectively, in all of the HTLV-1-carrying T-cell lines relative to the control cell line MOLT-4 (Table 1). When a correlation coefficient was calculated for the relative expression levels of the 108 genes in Table 1, 0.64, 0.60, and 0.96 were obtained between S1T and MT-2 cells, S1T and M8166 cells, and MT-2 and M8166 cells, respectively (data not shown). Thus, there was a positive correlation among the highly upregulated genes of the HTLV-1-carrying T-cell lines, indicating that our strategy may be applicable for identifying the molecules commonly overexpressed in ATL cells.

From the 108 genes, 11 genes of which products were considered to be expressed on the cell surface were listed in Fig. 2. These include the genes of tumor necrosis factor (TNF) ligand superfamily member 7 (CD70), major histocompatibility complex class II (MHC II) DRβ3 (HLA-DR3B), glucose transporter member 8 (GLUT8), IL-21R (NILR), prostaglandin E receptor 4 subtype EP4 (EP4), IL-4 receptor α chain isoform a (CD124), dodecenoyl-coenzyme A δ isomerase (CD79A), CD151 antigen (GP27), TNF superfamily member 10b isoform 1 (DR5), semaphorin 4C (SEMAI), and MHC I F (HLAF). Above all, the expression of the CD70 gene was enhanced more than 1,000-fold in all of the HTLV-1-carrying T-cell lines (Table 1 and Fig. 2). Therefore, we examined whether such

TABLE 1. Genes upregulated more than 10-fold in all of the HTLV-1-carrying T-cell lines compared with the HTLV-1-negative T-cell line MOLT-4[a]

Accession no.	Symbol	Relative expression level (fold change)			Gene product
		S1T	MT-2	M8166	
NM_138410	CKLFSF7	1,886.6 ± 188.7	293.0 ± 31.0	113.3 ± 19.9	CKLF-like MARVEL transmembrane domain containing 7 isoform a
NM_001252	CD70	1,375.3 ± 137.5	2,635.3 ± 263.5	2,594.8 ± 259.5	Tumor necrosis factor ligand superfamily, member 7
NM_005572	FPL	769.8 ± 88.2	822.0 ± 155.1	1,361.6 ± 136.2	Lamin A/C isoform 2
NM_004364	CEBP	539.9 ± 191.3	87.2 ± 8.7	56.9 ± 19.8	CCAAT/enhancer binding protein α
NM_022555	HLA-DR3B	474.0 ± 93.8	14.4 ± 4.9	54.0 ± 45.3	MHC II, DRβ3 precursor
NM_004364	CEBP	468.8 ± 144.7	72.8 ± 7.3	47.1 ± 17.4	CCAAT/enhancer binding protein alpha
NM_002304	NM_002304	336.0 ± 78.3	172.3 ± 36.6	135.3 ± 16.4	
NM_002166	GIG8	331.2 ± 33.1	265.4 ± 31.0	47.3 ± 24.0	Inhibitor of DNA binding 2
NM_024644	FLJ21802	325.1 ± 32.5	108.8 ± 18.0	107.3 ± 35.1	Chromosome 14 open reading frame 169
NM_015392	CAB	275.4 ± 27.5	130.9 ± 13.1	23.4 ± 2.3	Neural proliferation 1, differentiation and control
NM_014580	GLUT8	221.3 ± 22.1	93.3 ± 13.0	116.4 ± 11.8	Solute carrier family 2, (facilitated glucose transporter) member 8
NM_024710	TMEM101	217.8 ± 37.6	228.6 ± 54.0	245.8 ± 66.3	Isochorismatase domain containing 2
NM_015691	BM042	204.4 ± 20.4	80.5 ± 8.0	34.5 ± 7.7	WWC family member 3
NM_015892	GALNAC4S-6ST	178.9 ± 18.2	40.5 ± 6.8	37.0 ± 3.8	B-cell RAG-associated protein
NM_001017535	NR1I1	140.8 ± 42.1	178.1 ± 81.8	109.3 ± 66.6	Vitamin D (1,25-dihydroxyvitamin D3) receptor
NM_033518	SN2	113.5 ± 26.6	31.5 ± 11.6	58.5 ± 22.2	Amino acid transport system N2
NM_181078	NILR	112.5 ± 11.3	127.1 ± 25.3	178.5 ± 17.8	IL-21 receptor precursor
NM_012081	ELL2	112.4 ± 23.2	52.9 ± 5.3	19.7 ± 2.0	Elongation factor 2, RNA polymerase II
	ENST00000297871	102.3 ± 10.2	82.4 ± 8.2	95.9 ± 9.6	
NM_004737	MDC1D	97.8 ± 15.4	15.8 ± 1.7	106.7 ± 26.4	Like glycosyltransferase
NM_139346	AMPH2	83.6 ± 8.4	129.0 ± 12.9	119.6 ± 12.6	Bridging integrator 1 isoform 8
NM_022121	THW	74.0 ± 7.4	29.3 ± 3.0	65.1 ± 6.6	PERP, TP53 apoptosis effector
NM_014580	GLUT8	71.7 ± 7.2	26.0 ± 3.1	31.0 ± 3.1	Solute carrier family 2, (facilitated glucose transporter) member 8
NM_004350	AML2	67.8 ± 6.8	24.9 ± 2.5	61.0 ± 6.1	Runt-related transcription factor 3 isoform 1
NM_012465	KIAA0932	65.1 ± 13.3	24.5 ± 7.7	20.2 ± 2.7	Tolloid-like 2
NM_000447	AD4	64.6 ± 9.4	87.4 ± 19.1	58.6 ± 8.1	Presenilin 2 isoform 1
NM_016010	CGI-62	63.1 ± 6.3	24.6 ± 2.5	23.5 ± 2.4	Hypothetical protein LOC51101
NM_000447	AD4	62.2 ± 12.0	90.9 ± 19.7	57.1 ± 11.1	Presenilin 2 isoform 1
NM_000786	LDM	60.9 ± 8.1	59.2 ± 11.6	63.0 ± 6.3	Cytochrome P450, family 51
NM_005658	EBI6	54.6 ± 35.4	85.3 ± 14.2	165.7 ± 71.1	TNF receptor-associated factor 1
NM_025195	C8FW	53.8 ± 19.9	170.5 ± 17.1	29.9 ± 3.7	G-protein-coupled receptor-induced protein
NM_002306	GAL3	52.1 ± 5.2	133.4 ± 14.6	81.8 ± 11.0	Galectin 3
AK057088	AK057088	51.8 ± 5.2	11.4 ± 1.1	20.4 ± 2.0	
NM_000786	LDM	50.9 ± 7.1	49.2 ± 11.5	52.6 ± 5.3	Cytochrome P450, family 51
NM_000958	EP4	50.3 ± 10.5	22.7 ± 4.6	43.0 ± 7.0	Prostaglandin E receptor 4, subtype EP4
NM_177925	MGC921	48.9 ± 4.9	134.3 ± 13.4	132.5 ± 13.3	H2A histone family, member J isoform 1
NM_003254	EPA	48.0 ± 15.7	20.1 ± 2.7	10.9 ± 3.2	Tissue inhibitor of metalloproteinase 1 precursor
NM_018094	GST2	47.4 ± 5.0	68.6 ± 6.9	68.1 ± 7.2	Peptide chain release factor 3
BC018597	TEX264	43.8 ± 4.4	51.8 ± 5.2	74.4 ± 10.0	
	THC2440229	43.7 ± 9.9	13.5 ± 4.2	11.3 ± 3.1	
NM_002200	IRF5	43.7 ± 5.3	229.9 ± 23.0	48.9 ± 7.3	Interferon regulatory factor 5 isoform a
NM_014178	amisyn	38.5 ± 3.9	200.4 ± 32.5	30.6 ± 3.1	Amisyn
NM_014417	JFY1	38.4 ± 9.4	82.8 ± 14.8	118.3 ± 49.0	BCL2 binding component 3
NM_000199	HSS	37.6 ± 4.7	10.5 ± 1.0	12.8 ± 1.4	*N*-Sulfoglucosamine sulfohydrolase (sulfamidase)
AK090416	RXRA	37.3 ± 8.1	12.3 ± 4.1	27.9 ± 10.2	FLJ00318 protein
NM_000418	CD124	37.2 ± 6.2	43.8 ± 4.4	29.6 ± 9.7	Interleukin 4 receptor α chain isoform a precursor
NM_015111	N4BP3	36.5 ± 5.5	14.2 ± 1.4	27.5 ± 2.9	Nedd4 binding protein 3
NM_015459	DKFZP564J0863	34.8 ± 6.6	26.2 ± 2.6	18.5 ± 5.4	Hypothetical protein LOC25923
NM_018664	SNFT	34.7 ± 3.5	24.6 ± 2.5	11.7 ± 2.5	Jun dimerization protein p21SNFT
NM_013385	CYT4	34.1 ± 3.4	16.2 ± 4.7	107.6 ± 34.4	Pleckstrin homology, Sec7, and coiled-coil domains 4
NR_002323	TUG1	33.4 ± 3.3	30.3 ± 3.0	30.1 ± 5.2	
BC004219	MGC4604	33.1 ± 3.3	21.0 ± 2.1	13.0 ± 3.2	1-Acylglycerol-3-phosphate *O*-acyltransferase 3
BC035647	HLA-B	33.0 ± 6.3	52.4 ± 5.2	36.3 ± 5.7	
NM_006035	MRCKB	32.0 ± 3.2	65.7 ± 6.6	74.0 ± 7.4	CDC42-binding protein kinase β
NM_001919	CD79A	31.8 ± 3.2	15.6 ± 1.7	27.2 ± 4.0	Dodecenoyl-coenzyme A δ isomerase precursor
BQ189193	ICOSLG	31.8 ± 14.2	30.1 ± 3.8	72.7 ± 7.3	
	THC2401087	31.2 ± 3.1	42.5 ± 4.2	14.6 ± 4.0	
NM_001852	MED	30.7 ± 6.6	172.2 ± 33.3	52.9 ± 5.3	α2 type IX collagen
NM_004357	GP27	30.0 ± 4.4	34.0 ± 3.4	14.5 ± 4.5	CD151 antigen

Continued on facing page

TABLE 1—*Continued*

Accession no.	Symbol	Relative expression level (fold change)			Gene product
		S1T	MT-2	M8166	
NM_006509	I-REL	29.9 ± 3.0	65.0 ± 6.5	43.5 ± 5.1	Reticuloendotheliosis viral oncogene homolog B
AK096677	AK096677	29.2 ± 3.8	29.7 ± 7.2	73.3 ± 36.4	
NM_024758	FLJ23384	27.7 ± 4.5	23.1 ± 5.6	13.6 ± 2.1	Agmatine ureohydrolase (agmatinase)
AK021777	FLJ00205	25.8 ± 2.6	16.8 ± 1.7	19.9 ± 2.0	GalNAc transferase 10 isoform b
NM_001953	TP	25.2 ± 2.5	43.2 ± 4.3	30.8 ± 5.9	Endothelial cell growth factor 1 (platelet-derived)
NM_020731	AHH	24.8 ± 5.3	10.1 ± 1.6	99.4 ± 42.5	Arylhydrocarbon receptor repressor
NM_002413	GST2	24.6 ± 5.6	45.4 ± 4.6	51.5 ± 5.2	Microsomal glutathione *S*-transferase 2
NM_014383	Rog	24.3 ± 2.4	41.1 ± 4.1	12.5 ± 3.8	Testis zinc finger protein
NM_003928	MGC117411	24.2 ± 2.4	61.8 ± 7.1	35.8 ± 3.6	CAAX box 1
BX362492	BX362492	23.1 ± 4.0	26.3 ± 2.8	42.5 ± 11.0	
NM_033375	myr2	20.8 ± 2.9	45.4 ± 8.2	48.5 ± 8.3	Myosin IC
NM_213589	LPD	20.6 ± 2.3	14.9 ± 3.5	24.8 ± 3.1	Ras association and pleckstrin homology domains 1 isoform 2
NM_004838	HOMER-3	20.3 ± 2.0	193.6 ± 23.6	84.5 ± 15.8	Homer 3, neuronal immediate early gene
	A_23_P370707	18.2 ± 7.7	42.1 ± 4.2	30.1 ± 7.0	
AB033060	AHH	17.9 ± 3.9	12.2 ± 1.2	114.8 ± 22.4	Arylhydrocarbon receptor repressor
BC024020	VMP1	17.6 ± 2.6	39.6 ± 4.0	22.8 ± 6.0	Transmembrane protein 49
NM_023076	FLJ23360	17.6 ± 3.1	21.2 ± 4.0	20.5 ± 2.8	Hypothetical protein LOC65259
AK097976	DLEU2	17.2 ± 3.1	22.5 ± 5.3	13.6 ± 8.3	
NM_003842	DR5	16.7 ± 1.7	32.9 ± 4.0	37.2 ± 3.7	TNF receptor superfamily, member 10b isoform 1 precursor
NM_024646	ZYG11	16.5 ± 1.7	11.1 ± 1.1	15.1 ± 1.5	Zyg-11 homolog B
AK092921	HLA-B	16.3 ± 1.6	25.7 ± 2.6	19.9 ± 2.0	
NM_022152	RECS1	16.2 ± 1.6	13.6 ± 2.9	14.7 ± 3.0	Transmembrane BAX inhibitor motif containing 1
AA451906	BIN1	15.4 ± 1.5	18.2 ± 2.0	17.3 ± 1.7	
NM_018370	DRAM	15.3 ± 2.5	80.9 ± 14.7	41.6 ± 10.8	Damage-regulated autophagy modulator
NM_005514	HLA B	15.2 ± 1.7	32.3 ± 3.2	28.0 ± 4.9	MHC I, B
	THC2403644	14.9 ± 4.4	17.5 ± 5.9	15.0 ± 5.0	
NM_000152	LYAG	14.7 ± 1.5	15.8 ± 2.4	13.0 ± 2.1	Acid α-glucosidase preproprotein
	ENST00000355804	14.4 ± 1.4	23.7 ± 2.8	13.1 ± 1.7	
NM_001613	ACTSA	14.4 ± 1.6	35.3 ± 5.4	22.3 ± 2.3	α2 actin
NM_018370	DRAM	14.3 ± 2.3	73.3 ± 12.4	33.9 ± 7.7	Damage-regulated autophagy modulator
	A_24_P101771	14.0 ± 1.5	21.3 ± 2.2	19.3 ± 3.3	
NM_017789	SEMAI	13.9 ± 1.7	20.4 ± 2.5	33.9 ± 13.8	Semaphorin 4C
NM_002502	LYT10	13.3 ± 4.3	15.4 ± 1.0	45.9 ± 2.8	Nuclear factor of κ light polypeptide gene enhancer in B cells 2 (p49/p100)
NM_031419	IKBZ	12.6 ± 4.6	37.1 ± 4.9	134.0 ± 62.5	Nuclear factor of κ light polypeptide gene enhancer in B cells inhibitor, ζ isoform b
NM_015516	TSK	12.5 ± 1.2	12.7 ± 1.3	12.2 ± 1.2	Tsukushi
CR594843	HLA-B	12.2 ± 1.2	11.5 ± 1.2	10.1 ± 1.9	
NM_018950	HLAF	12.1 ± 1.8	16.7 ± 1.7	13.7 ± 2.0	MHC I, F precursor
NM_024567	PBHNF	12.0 ± 1.9	15.3 ± 3.0	17.0 ± 2.8	Homeobox containing 1
NM_003764	FHL4	12.0 ± 2.1	14.0 ± 1.4	11.7 ± 4.4	Syntaxin 11
	THC2276547	11.9 ± 1.3	16.8 ± 4.7	30.9 ± 9.6	
CA431756	CTTN	11.3 ± 1.4	13.8 ± 1.5	12.8 ± 3.1	
CR608347	HLA-B	11.0 ± 1.2	16.5 ± 1.4	12.7 ± 1.9	
NM_005261	KIR	11.0 ± 4.5	96.2 ± 9.6	97.3 ± 56.7	GTP-binding mitogen-induced T-cell protein
NM_130446	FLJ00029	11.0 ± 1.2	11.6 ± 3.5	13.6 ± 7.1	Kelch-like 6
NM_017789	SEMAI	10.9 ± 1.1	16.4 ± 1.6	24.6 ± 10.4	Semaphorin 4C
BC037255	LOC389634	10.6 ± 1.1	16.8 ± 3.0	21.3 ± 6.4	Hypothetical protein LOC389634
AF009619	CASH	10.6 ± 1.7	16.4 ± 3.3	85.1 ± 38.2	CASP8 and FADD-like apoptosis regulator
NM_006674	P5-1	10.5 ± 1.2	58.0 ± 5.8	91.4 ± 9.3	HLA complex P5
NR_001434	HLAHP	10.2 ± 1.0	15.7 ± 1.6	18.5 ± 2.4	

[a] The genes of which expression levels were more than 10-fold in all of the three HTLV-1-carrying T-cell lines (S1T, MT-2, and M8166) compared with the control T-cell line (MOLT-4) with statistical significance ($P < 0.05$) are listed and sorted by the expression level in S1T cells. All data represent means ± standard deviations for three independent microarray experiments.

high upregulation of the CD70 gene was reflected in the expression of the CD70 molecule on the surfaces of the cell lines.

CD70 expression in HTLV-1-carrying T-cell lines. As shown in Fig. 3, MOLT-4 cells did not express CD70 on their surfaces, whereas this molecule was highly expressed on the HTLV-1-carrying cell T-lines S1T, MT-2, M8166, and MT-4. Like the case for MOLT-4 cells, CD70 expression was scarcely observed for other HTLV-1-negative T-cell lines (CEM, Jurkat, and the monocytic cell lines U937 and HL-60), suggesting that CD70 is selectively expressed in HTLV-1-carrying T-cell lines. Such selectivity was also confirmed by the analysis of these cell lines for the expression of CD124, IL-21R, and CD151 on the surface. The gene expression of not only CD70 but also CD124, IL-21R, and CD151 was highly upregulated in all of the

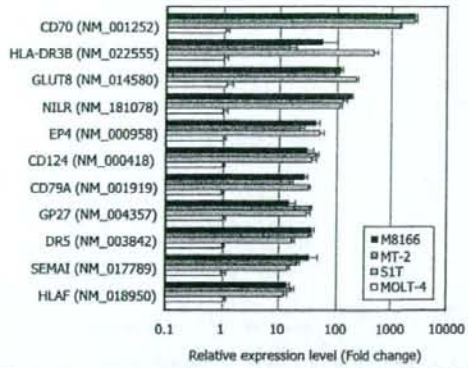

FIG. 2. Genes upregulated more than 10-fold in the HTLV-1-carrying T-cell lines S1T, MT-2, and M8166 compared with the genes in HTLV-1-negative T-cell line MOLT-4. The genes of which products are considered to be expressed on the cell surface are shown. All data represent means ± standard deviations (error bars) for three independent microarray experiments.

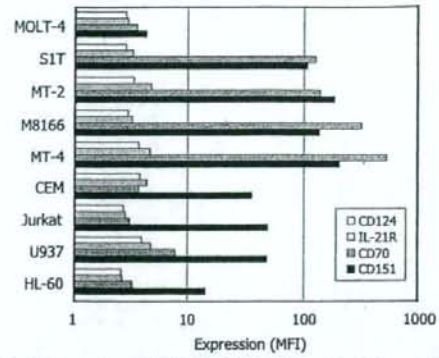

FIG. 4. Expression of CD124, IL-21R, CD70, and CD151 on various cell lines. The cells were strained with appropriate MAbs described in Materials and Methods and analyzed by laser flow cytometry. The expression level of each molecule is expressed as mean fluorescence intensity (MFI).

HTLV-1-carrying T-cell lines (Table 1 and Fig. 2). However, there was no significant difference of CD124 and IL-21R expression among the nine cell lines (Fig. 4). Like CD70, CD151 was strongly expressed on the HTLV-1-carrying T-cell lines compared with MOLT-4 cells, yet this molecule was also highly expressed on CEM, Jurkat, and U937 cells, indicating that CD151 expression was not selective enough to HTLV-1-carrying T-cell lines.

CD70 expression in leukemic cells from ATL patients. To determine whether CD70 is a potential target for anti-ATL

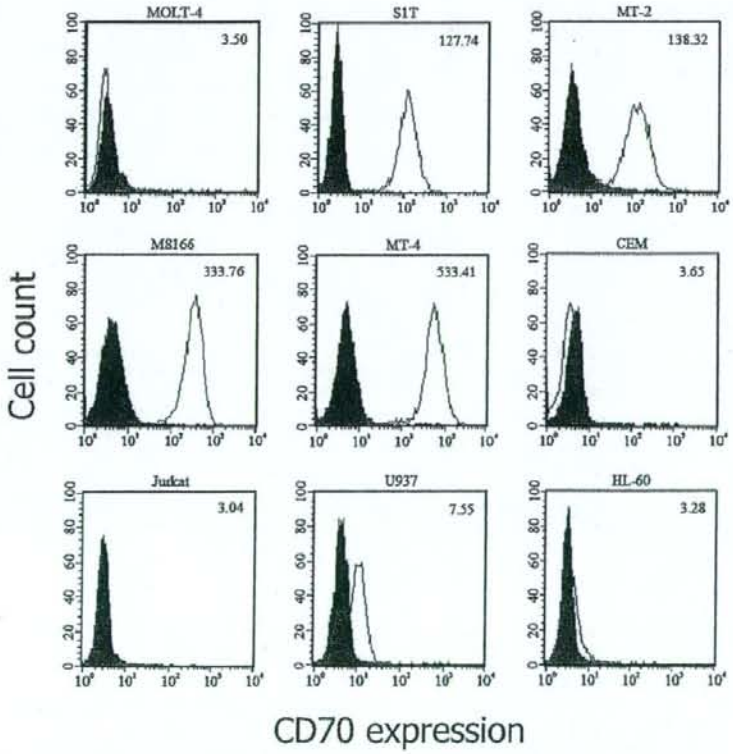

FIG. 3. CD70 expression on various cell lines. The cells were strained with an anti-human CD70 MAb (white histogram) or its isotype control MAb (gray histogram) and analyzed by laser flow cytometry. The number in each histogram indicates the mean fluorescence intensity of the cells.

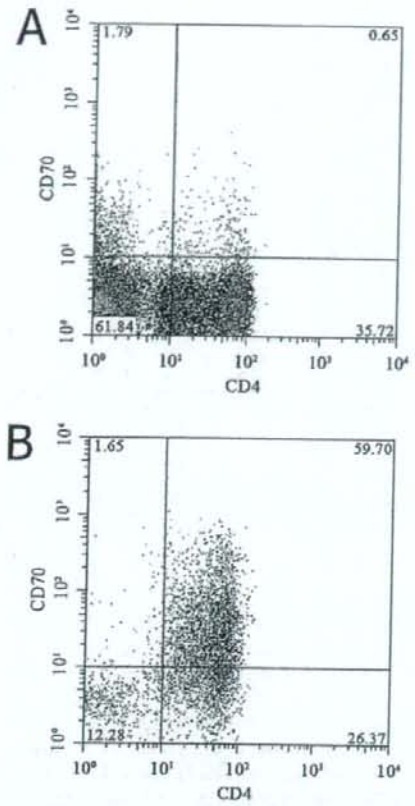

FIG. 5. CD70 expression on CD4$^+$ T cells isolated from healthy donors and ATL patients. PBMCs were isolated from (A) an HTLV-1-negative healthy donor (HD-1 in Table 1) and (B) an acute-type ATL patient (ATL-1 in Table 1). The cells were examined for their CD4 and CD70 expression by laser flow cytometry after being gated by their forward and side scattering intensities. The percentage of CD70$^+$ cells among CD4$^+$ cells was calculated by the following formula: percentage of upper right quadrant/(percentage of upper right quadrant + percentage of lower right quadrant).

MAb therapy, the selective expression of CD70 has to be demonstrated in the primary ATL cells isolated from patients. When PBMCs were isolated from an HTLV-1-negative healthy donor and examined for their CD4 and CD70 expression by laser flow cytometry, a small number (approximately 1.8%) of CD4$^+$ cells, which were regarded as T cells because of their being gated by forward and side scattering intensities, were CD70$^+$ (Fig. 5A). Under the same conditions, 69.2% of the CD4$^+$ cells isolated from an acute-type ATL patient were CD70$^+$ (Fig. 5B). Therefore, we extended the analysis to PBMCs obtained from an additional five HTLV-1-negative healthy donors and five acute-type ATL patients. As shown in Table 2, the average numbers of CD70$^+$ cells were 3.2 and 79.3% of the total CD4$^+$ T cells obtained from the healthy donors and ATL patients, respectively, which was statistically significant ($P < 0.00095$). In contrast, there was no practical difference of CD70 expression on B cells and monocytes between healthy donors and ATL patients. Although certain difference of CD70 expression was observed for CD8$^+$ T-cells, it was not statistically significant. Furthermore, difference of CD70 expression on CD8$^+$ T cells, B cells, and monocytes varied from one patient to another. These results suggest that CD70 is predominantly expressed on the CD4$^+$ T cells, presumably leukemia cells, from acute-type ATL patients.

Effect of anti-human CD70 MAb on ATL cells. When S1T and MOLT-4 cells were incubated with a commercially available anti-human CD70 MAb, the MAb did not affect the proliferation of these cell lines at a concentration of 1 μg/ml during a 4-day incubation period (Fig. 6A). The effect of an anti-human CD70 MAb for the viability of primary ATL cells was also examined. No significant reduction of cell viability was observed at concentrations of up to 1 μg/ml for all of the PBMCs obtained from three different ATL patients (Fig. 6B).

DISCUSSION

Human oligonucleotide microarrays have been used to examine gene expression patterns of PBMCs infected with HTLV-1 (11), HTLV-1-transformed T-cell lines (8, 30), Jurkat cells expressing either p12I (26) or p30II (23), and the Jurkat cell line JPX-9 that can be induced to express higher levels of Tax-1 (27). In addition, activated PBMC cDNA has been used in subtraction hybridization studies with cDNA from cultured ATL cells from a patient (33). The complexity of the data from these studies and differences in chip composition preclude a full definition of genes that are affected by viral infection. However, there is a consensus on the expression of some cellular genes. Enhanced expression of cell cycle and antiapoptotic genes includes the cyclin B1, p21WAF1/CIP1, and Bcl-X(L) genes, confirming prior biological/biochemical findings (1, 5, 25, 28). In contrast, caspase-8 appears to be consistently downregulated. Among the interleukins and their receptors, the upregulation of IL-2Rα, but not IL-2, is also consistently detected. In contrast, IL-15Rα appears to be upregulated in only some HTLV-1-infected T-cell lines and PBMCs. Similarly, IL-15 is not upregulated in all cell lines and IL-15 expression does not appear to be induced by Tax-1 in Jurkat cells.

There is a criticism that limited or biased information regarding the molecules selectively expressed in ATL cells will be obtained when HTLV-1-carrying T-cell lines, instead of primary ATL cells, are used for oligonucleotide microarray analysis (35). This criticism may be appropriate from one aspect, since such HTLV-1-carrying T-cell lines generally express the viral transactivator protein Tax that considerably affects viral and cellular gene expression. In fact, our study demonstrated that MT-2 and M8166 cells strongly expressed Env-Tax fusion protein and Tax, respectively (Fig. 1B). Both cell lines were established by cocultivation of healthy human cord blood T cells with ATL cells (24). Therefore, it is not surprising that unlike primary ATL cells, these in vitro-transformed T-cell lines still retain functional Tax. This may be a reason for the high correlation coefficient (0.96) in relative expression levels of the 108 genes between MT-2 and M8166 cells (Table 1). On the other hand, S1T cells were directly established from primary ATL cells by cultivation with IL-2 (2). Consequently, S1T cells did not express *env* or *tax* gene as well as Env or Tax (Fig. 1).

TABLE 2. CD70 expression in PBMCs isolated from healthy donors and ATL patients[a]

Donor	WBC[b] (cells/mm^3)	Expression on indicated marker-positive cells (%)[c]						
		$CD3^+$ $CD70^+$	$CD4^+$ $CD70^+$	$CD4^+$ $CD25^+$	$CD4^+$ $CD25^+$ $CD70^+$	$CD8^+$ $CD70^+$	$CD19^+$ $CD70^+$	$CD14^+$ $CD70^+$
HD-1		2.6	1.8	ND	0.3	0.6	16.5	0
HD-2		2.9	2.7	1.5	0.4	4.2	17.9	0.1
HD-3		2.4	1.9	3.6	0.4	0.2	13.6	0
HD-4		6.3	4.2	7.1	1.2	0.6	20.3	0.5
HD-5		9.4	5.8	7.7	1.3	3.9	15.8	0.3
HD-6		5.5	2.8	14.2	1.3	ND	27.5	0.3
ATL-1	414,000	67.5	69.2	73.6	56.6	ND	14.5	0
ATL-2	28,300	98.0	98.6	97.5	98.5	91.3	18.3	0
ATL-3	296,000	66.6	84.3	40.6	36.9	0	0	0
ATL-4	9,100	99.1	98.7	58.7	58.8	84.6	8.7	0.5
ATL-5		81.6	31.5	10.4	5.7	74.6	21.5	33.9
ATL-6		94.3	93.4	73.1	69.6	24.5	16.7	1.5

[a] PBMCs obtained from healthy donors (HD) and acute-type ATL patients were stained with appropriate MAbs (see Materials and Methods). After staining, the cells were analyzed by laser flow cytometry.

[b] WBC, white blood cell count.

[c] Mean ± standard deviation values for healthy donors were 4.9 ± 2.8 for $CD3^+$ $CD70^+$ cells, 3.2 ± 1.5 for $CD4^+$ $CD70^+$ cells, 6.8 ± 4.8 for $CD4^+$ $CD25^+$ cells, 0.8 ± 0.5 for $CD4^+$ $CD25^+$ $CD70^+$ cells, 1.9 ± 2.0 for $CD8^+$ $CD70^+$ cells, 18.6 ± 4.9 for $CD19^+$ $CD70^+$ cells, and 0.2 ± 0.2 for $CD14^+$ $CD70^+$ cells. Mean ± standard deviation values for ATL patients were 84.5 ± 14.9 for $CD3^+$ $CD70^+$ cells (statistically significant [$P < 0.01$] by t test), 79.3 ± 25.9 for $CD4^+$ $CD70^+$ cells (statistically significant [$P < 0.01$] by t test), 59.0 ± 30.3 for $CD4^+$ $CD25^+$ cells (statistically significant [$P < 0.01$] by t test), 54.4 ± 31.2 for $CD4^+$ $CD25^+$ $CD70^+$ cells (statistically significant [$P < 0.01$] by t test), 55.0 ± 40.4 for $CD8^+$ $CD70^+$ cells, 13.3 ± 7.8 for $CD19^+$ $CD70^+$ cells, and 6.0 ± 13.7 for $CD14^+$ $CD70^+$ cells. ND, not determined.

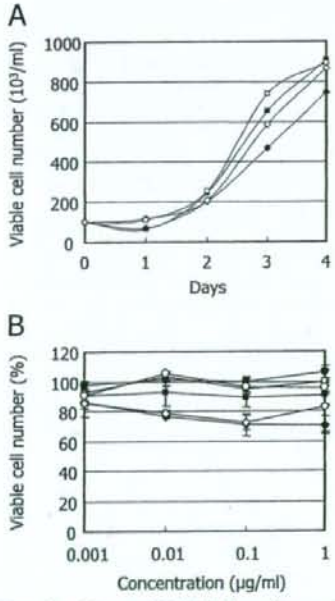

FIG. 6. Effect of anti-human CD70 MAb on the growth and viability of ATL cells. (A) S1T (diamonds) and MOLT-4 (squares) cells were incubated with an anti-CD70 MAb (filled symbols) or its isotype-matched control MAb (open symbols) at a concentration of 1 μg/ml. After a 4-day incubation, the number of viable cells was determined by trypan blue exclusion. (B) PBMCs obtained from three different ATL patients (circles, squares, and diamonds) were incubated with an anti-CD70 MAb (closed symbols) or its isotype-matched control MAb (open symbols) at various concentrations. After a 24-h incubation, the number of viable cells was determined by the MTT method. Error bars indicate standard deviations.

In this point of view, if HTLV-1-carrying T-cell lines with totally different origins could be included for oligonucleotide microarray analysis, it would become an efficient approach to determining the molecules selectively expressed in ATL cells. In the present study, 108 genes were found to be upregulated more than 10-fold in different HTLV-1-carrying T-cell lines relative to a control T-cell line (Table 1). Among them, tremendous (more than 1,000-fold) upregulation was observed for the CD70 gene, of which product should be expressed on the cell surface (Fig. 2). In fact, the CD70 molecule was strongly and selectively expressed on various HTLV-1-carrying T-cell lines and $CD4^+$ T-cells obtained from ATL patients but not on HTLV-1-negative T-cell lines, monocytic cell lines, or $CD4^+$ T-cells obtained from HTLV-1-negative healthy donors (Fig. 4 and 5 and Table 2).

CD70 is the only known ligand for its receptor CD27 that belongs to the TNF receptor superfamily 7. In general, this molecule is expressed on strongly activated T and B cells (4) and some hematological malignancies, such as non-Hodgkin's lymphoma (42). In fact, when PBMCs were isolated and stimulated with phytohemagglutinin, approximately 18 and 32% of the cells became $CD70^+$ after 7 and 12 days of cultivation, respectively (data not shown). However, there has been no definitive report describing the selective expression of CD70 in ATL cells. CD70 is also highly expressed on some solid tumors, including renal cell carcinoma (9, 17) and glioblastoma (6, 43). In contrast, CD70 expression is highly restricted in normal tissues (19). Therefore, CD70 has been considered to be an attractive target of MAbs and MAb-drug conjugates for selective anticancer therapy. It was recently shown that the administration of an engineered anti-CD70 MAb significantly prolonged the survival of severe combined immunodeficient mice bearing $CD70^+$-disseminated human non-Hodgkin's lymphoma xenografts (22). In this study, treatment with control IgG did not prolong median survival (21 days). In contrast, median survival was increased to 72 days when the mice were

treated with the anti-CD70 MAb at a dose of 4 mg/kg of body weight. Furthermore, anti-CD70 antibody-drug conjugates were effective against tumor growth in mice bearing human renal cell carcinoma xenografts (6). These results suggest that irrespective of drug conjugates, anti-CD70 MAbs deserve to be investigated for their anticancer activities against ATL in vitro and in vivo.

In addition to CD70, we have also identified 10 genes of which products should be highly expressed on the HTLV-1-carrying T-cell lines (Fig. 2). Among these, three molecules, CD124, IL-21R, and CD151, could be evaluated for their expressions on various cell lines, since MAbs for these molecules were commercially available. CD151 was indeed highly expressed on the HTLV-1-carrying T-cell lines, yet it was also expressed in other T-cell and monocytic cell lines, except MOLT-4 (Fig. 4). CD151 is a member of the tetraspanin family and is a broadly expressed molecule. It is also noted for its strong molecular associations with integrins (44). CD151 was initially identified as a marker of human acute myeloid leukemia cells, platelets, and vascular endothelial cells (3). The upregulation of the CD151 gene in HTLV-1-carrying T-cell lines has already been reported and investigated for its pathological role (13, 14). Our microarray analysis has confirmed these reports. Since CD151 is broadly expressed by a variety of cell types (36), it does not seem to be a suitable target for anticancer therapy with MAbs. Further studies are in progress to identify other molecules selectively expressed on primary ATL cells obtained from patients.

At present, there is no evidence indicating that commercially available anti-CD70 MAbs are capable of inhibiting cell proliferation or inducing apoptosis of primary ATL cells obtained from patients as well as the S1T cells (Fig. 6). It is possible that these anti-CD70 MAbs are not optimized to exert their biological functions and may be required for structural modification. However, a company in New Jersey has recently obtained permission from the U.S. Food and Drug Administration to use a fully human MAb directed against CD70 in a phase I clinical trial for treatment of clear cell renal cell carcinoma (Medarex). Considering this fact and the poor prognosis and lack of curative therapy for ATL, CD70 should be further perused as a potential target in anticancer therapy against ATL.

ACKNOWLEDGMENTS

The anti-p40 Tax monoclonal antibody Lt-4 was kindly provided by Y. Tanaka (University of the Ryukyus, Okinawa, Japan). We thank T. Uto and M. Tokitou for their technical assistance.

This work was supported by a grant from the Frontier Science Research Center, Kagoshima University, and a grant-in-aid for Scientific Research (B) from the Japan Society for the Promotion of Science (grant no. 19390153).

REFERENCES

1. **Akagi, T., H. Ono, and K. Shimotohno.** 1996. Expression of cell-cycle regulatory genes in HTLV-I infected T-cell lines: possible involvement of Tax1 in the altered expression of cyclin D2, p18(Ink4) and p21(Waf1/Cip1/Sdi1). Oncogene **12**:1645–1652.
2. **Arima, N., J. A. Molitor, M. R. Smithe, J. H. Kim, Y. Daitoku, and W. C. Greene.** 1991. Human T-cell leukemia virus type I Tax induces expression of the Rel-related family of κB enhancer-binding proteins: evidence for a pretranslational component of regulation. J. Virol. **65**:6892–6899.
3. **Ashman, L. K., G. Aylett, P. Mehrabani, L. Bendall, S. Niutta, A. C. Cambareri, S. R. Cole, and M. Berndt.** 1991. The murine monoclonal antibody, 14A2.H1, identifies a novel platelet surface antigen. Br. J. Haematol. **79**:263–270.
4. **Borst, J., J. Hendriks, and Y. Xiao.** 2005. CD27 and CD70 in T cell and B cell activation. Curr. Opin. Immunol. **17**:275–281.
5. **Cereseto, A., J. C. Mulloy, and G. Franchini.** 1996. Insights on the pathogenicity of human T-lymphotropic/leukemia virus types I and II. J. Acquir. Immune Defic. Syndr. Hum. Retrovirol. **13**(Suppl. 1):S69–S75.
6. **Chahlavi, A., P. Rayman, A. L. Richmond, K. Biswas, R. Zhang, M. Vogelbaum, C. Tannenbaum, G. Barnett, and J. H. Finke.** 2005. Glioblastomas induce T-lymphocyte death by two distinct pathways involving gangliosides and CD70. Cancer Res. **65**:5428–5438.
7. **Choi, Y. L., K. Tsukasaki, M. C. O'Neill, Y. Yamada, Y. Onimaru, K. Matsumoto, J. Ohashi, Y. Yamashita, S. Tsutsumi, R. Kaneda, S. Takada, H. Aburatani, S. Kamihira, T. Nakamura, M. Tomonaga, and H. Mano.** 2007. A genomic analysis of adult T-cell leukemia. Oncogene **26**:1245–1255.
8. **de La Fuente, C., L. Deng, F. Santiago, L. Arce, L. Wang, and F. Kashanchi.** 2000. Gene expression array of HTLV type 1-infected T cells: up-regulation of transcription factors and cell cycle genes. AIDS Res. Hum. Retrovir. **16**:1695–1700.
9. **Diegmann, J., K. Junker, B. Gerstmayer, A. Bosio, W. Hindermann, J. Rosenhahn, and F. von Eggeling.** 2005. Identification of CD70 as a diagnostic biomarker for clear cell renal cell carcinoma by gene expression profiling, real-time RT-PCR and immunohistochemistry. Eur. J. Cancer **41**:1794–1801.
10. **Gessain, A., F. Barin, J. C. Vernant, O. Gout, L. Maurs, A. Calender, and G. de Thé.** 1985. Antibodies to human T-lymphotropic virus type-I in patients with tropical spastic paraparesis. Lancet **2**:407–410.
11. **Harhaj, E. W., L. F. Good, G. T. Xiao, and S. C. Sun.** 1999. Gene expression profiles in HTLV-I-immortalized T cells: deregulated expression of genes involved in apoptosis regulation. Oncogene **18**:1341–1349.
12. **Harris, M.** 2004. Monoclonal antibodies as therapeutic agents for cancer. Lancet Oncol. **5**:292–302.
13. **Hasegawa, H., Y. Utsunomiya, K. Kishimoto, K. Yanagisawa, and S. Fujita.** 1996. SFA-1, a novel cellular gene induced by human T-cell leukemia virus type 1, is a member of the transmembrane 4 superfamily. J. Virol. **70**:3258–3263.
14. **Hasegawa, H., T. Nomura, K. Kishimoto, K. Yanagisawa, and S. Fujita.** 1998. SFA-1/PETA-3 (CD151), a member of the transmembrane 4 superfamily, associates preferentially with $\alpha_3\beta_1$ integrin and regulates adhesion of human T cell leukemia virus type 1-infected T cells to fibronectin. J. Immunol. **161**:3087–3095.
15. **Iannello, A., and A. Ahmad.** 2005. Role of antibody-dependent cell-mediated cytotoxicity in the efficacy of therapeutic anti-cancer monoclonal antibodies. Cancer Metastasis Rev. **24**:487–499.
16. **Ishikawa, T.** 2003. Current status of therapeutic approaches to adult T-cell leukemia. Int. J. Hematol. **78**:304–311.
17. **Junker, K., W. Hindermann, F. von Eggeling, J. Diegmann, K. Haessler, and J. Schubert.** 2005. CD70: a new tumor specific biomarker for renal cell carcinoma. J. Urol. **173**:2150–2153.
18. **Kobayashi, N., H. Konishi, H. Sabe, K. Shigesada, T. Noma, T. Honjo, and M. Hatanaka.** 1984. Genomic structure of HTLV (human T-cell leukemia virus): detection of defective genome and its amplification in MT-2 cells. EMBO J. **3**:1339–1343.
19. **Law, C. L., K. A. Gordon, B. E. Toki, A. K. Yamane, M. A. Hering, C. G. Cerveny, J. M. Petroziello, M. C. Ryan, L. Smith, R. Simon, G. Sauter, E. Oflazoglu, S. O. Doronina, D. L. Meyer, J. A. Francisco, P. Carter, P. D. Senter, J. A. Copland, C. G. Wood, and A. F. Wahl.** 2006. Lymphocyte activation antigen CD70 expressed by renal cell carcinoma is a potential therapeutic target for anti-CD70 antibody-drug conjugates. Cancer Res. **66**:2328–2337.
20. **Lin, M. Z., M. A. Teitell, and G. J. Schiller.** 2005. The evolution of antibodies into versatile tumor-targeting agents. Clin. Cancer Res. **11**:129–138.
21. **Marcus, R., and A. Hagenbeek.** 2007. The therapeutic use of rituximab in non-Hodgkin's lymphoma. Eur. J. Haematol. S. **67**:5–14.
22. **McEarchern, J. A., E. Oflazoglu, L. Francisco, C. F. McDonagh, K. A. Gordon, I. Stone, K. Klussman, E. Turcott, N. van Rooijen, P. Carter, I. S. Grewal, A. F. Wahl, and C. L. Law.** 2007. Engineered anti-CD70 antibody with multiple effector functions exhibits in vitro and in vivo antitumor activities. Blood **109**:1185–1192.
23. **Michael, B., A. M. Nair, H. Hiraragi, L. Shen, G. Feuer, K. Boris-Lawrie, and M. D. Lairmore.** 2004. Human T lymphotropic virus type-1 p30II alters cellular gene expression to selectively enhance signaling pathways that activate T lymphocytes. Retrovirology **1**:39.
24. **Miyoshi, I., I. Kubonishi, S. Yoshimoto, T. Akagi, Y. Ohtsuki, Y. Shiraishi, K. Nagata, and Y. Hinuma.** 1981. Type C virus particles in a cord T-cell line derived by co-cultivating normal human cord leukocytes and human leukaemic T cells. Nature **294**:770–771.
25. **Mori, N., M. Fujii, G. Cheng, S. Ikeda, Y. Yamasaki, Y. Yamada, M. Tomonaga, and N. Yamamoto.** 2001. Human T-cell leukemia virus type I tax protein induces the expression of anti-apoptotic gene Bcl-xL in human T-cells through nuclear factor-κB and c-AMP responsive element binding protein pathways. Virus Genes **22**:279–287.
26. **Nair, A., B. Michael, H. Hiraragi, S. Fernandez, G. Feuer, K. Boris-Lawrie, and M. Lairmore.** 2005. Human T lymphotropic virus type I accessory protein p12I modulates calcium-mediated cellular gene expression and enhances p300 expression in T lymphocytes. AIDS Res. Hum. Retrovir. **21**: 273–284.

27. **Ng, P. W., H. Iha, Y. Iwanaga, M. Bittner, Y. Chen, Y. Jiang, G. Gooden, J. M. Trent, P. Meltzer, K. T. Jeang, and S. L. Zeichner.** 2001. Genome-wide expression changes induced by HTLV-1 Tax: evidence for MLK-3 mixed lineage kinase involvement in Tax-mediated NF-κB activation. Oncogene **20**:4484–4496.
28. **Nicot, C., R. Mahieux, S. Takemoto, and G. Franchini.** 2000. Bcl-X(L) is up-regulated by HTLV-I and HTLV-II in vitro and in ex vivo ATLL samples. Blood **96**:275–281.
29. **Osame, M., K. Usuku, S. Izumo, N. Ijichi, H. Amitani, A. Igata, M. Matsumoto, and M. Tara.** 1986. HTLV-I associated myelopathy, a new clinical entity. Lancet **1**:10310–11032.
30. **Pise-Masison, C. A., M. Radonovich, R. Mahieux, P. Chatterjee, C. Whiteford, J. Duvall, C. Guillerm, A. Gessain, and J. N. Brady.** 2002. Transcription profile of cells infected with human T-cell leukemia virus type I compared with activated lymphocytes. Cancer Res. **62**:3562–3571.
31. **Proietti, F. A., A. B. Carneiro-Proietti, B. C. Catalan-Soares, and E. L. Murphy.** 2005. Global epidemiology of HTLV-I infection and associated diseases. Oncogene **24**:6058–6068.
32. **Reff, M. E., K. Carner, K. S. Chambers, P. C. Chinn, J. E. Leonard, R. Raab, R. A. Newman, N. Hanna, and D. R. Anderson.** 1994. Depletion of B cells in vivo by a chimeric mouse human monoclonal antibody to CD20. Blood **83**:435–445.
33. **Ruckes, T., D. Saul, J. Van Snick, O. Hermine, and R. Grassmann.** 2001. Autocrine antiapoptotic stimulation of cultured adult T-cell leukemia cells by overexpression of the chemokine I-309. Blood **98**:1150–1159.
34. **Salahuddin, S. Z., P. D. Markham, F. Wong-Staal, G. Franchini, V. S. Kalyanaraman, and R. C. Gallo.** 1983. Restricted expression of human T-cell leulemia-lymphoma virus (HTLV) in transformed human umbilical cord blood lymphocytes. Virology **129**:51–64.
35. **Sasaki, H., I. Nishikata, T. Shiraga, E. Akamatsu, T. Fukami, T. Hidaka, Y. Kubuki, A. Okayama, K. Hamada, H. Okabe, Y. Murakami, H. Tsubouchi, and K. Morishita.** 2005. Overexpression of a cell adhesion molecule, TSLC1, as a possible molecular marker for acute-type adult T-cell leukemia. Blood **105**:1204–1213.
36. **Sincock, P., G. Mayrhofer, and L. K. Ashman.** 1997. Localization of the transmembrane 4 superfamily (TM4SF) member PETA-3 (CD151) in normal human tissues: comparison with CD9, CD63, and α5β1 integrin. J. Histochem. Cytochem. **45**:515–525.
37. **Takatsuki, K.** 2005. Discovery of adult T-cell leukemia. Retrovirology **2**:16.
38. **Tanaka, Y., A. Yoshida, Y. Takayama, H. Tsujimoto, A. Tsujimoto, M. Hayami, and H. Tozawa.** 1990. Heterogeneity of antigen molecules recognized by anti-tax1 monoclonal antibody Lt-4 in cell lines bearing human T cell leukemia virus type I and related retroviruses. Jpn. J. Cancer Res. **81**:225–231.
39. **Taylor, G. P., and M. Matsuoka.** 2005. Natural history of adult T-cell leukemia/lymphoma and approaches to therapy. Oncogene **24**:6047–6057.
40. **Uchiyama, T., J. Yodoi, K. Sagawa, K. Takatsuki, and H. Uchino.** 1977. Adult T-cell leukemia: clinical and hematologic features of 16 cases. Blood **50**:481–492.
41. **Wang, X., H. Miyake, M. Okamoto, M. Saito, J. Fujisawa, Y. Tanaka, S. Izumo, and M. Baba.** 2002. Inhibition of the tax-dependent human T-lymphotropic virus type I replication in persistently infected cells by the fluoroquinolone derivative K-37. Mol. Pharmacol. **61**:1359–1365.
42. **Widney, D., G. Gundapp, J. W. Said, M. van der Meijden, B. Bonavida, A. Demidem, C. Trevisan, J. Taylor, R. Detels, and O. Martinez-Maza.** 1999. Aberrant expression of CD27 and soluble CD27 (sCD27) in HIV infection and in AIDS-associated lymphoma. Clin. Immunol. **93**:114–123.
43. **Wischhusen, J., G. Jung, I. Radovanovic, C. Beier, J. P. Steinbach, A. Rimner, H. Huang, J. B. Schulz, H. Ohgaki, A. Aguzzi, H. G. Rammensee, and M. Weller.** 2002. Identification of CD70-mediated apoptosis of immune effector cells as a novel immune escape pathway of human glioblastoma. Cancer Res. **62**:2592–2599.
44. **Wright, M. D., S. M. Geary, S. Fitter, G. W. Moseley, L. M. Lau, K. C. Sheng, V. Apostolopoulos, E. G. Stanley, D. E. Jackson, and L. K. Ashman.** 2004. Characterization of mice lacking the tetraspanin superfamily member CD151. Mol. Cell. Biol. **24**:5978–5988.

J. Biochem. 143, 833–839 (2008)
doi:10.1093/jb/mvn038

One-Step Purification of Lectins from Banana Pulp Using Sugar-Immobilized Gold Nano-Particles

Sachiko Nakamura-Tsuruta[1], Yuko Kishimoto[3], Tomoaki Nishimura[3] and Yasuo Suda[1,2,3,*]

[1]Venture Business Laboratory; [2]Department of Nanostructure and Advanced Materials, Kagoshima University, 1-21-40, Kohrimoto, Kagoshima 890-0065; and [3]SUDx-Biotec Corp., KIBC #461, 5-5-2, Minatojima-minami, Chuo-ku, Kobe 650-0047, Japan

Received December 24, 2007; accepted February 29, 2008; published online March 15, 2008

To obtain lectins without tedious purification steps, we developed a convenient method for a one-step purification of lectins using sugar-immobilized gold nano-particles (SGNPs). Proteins in crude extracts from plant materials were precipitated with 60% ammonium sulphate, and the precipitate was re-dissolved in a small volume of phosphate buffer. The resultant solution was then mixed with appropriate SGNPs under an optimized condition. After incubating overnight at 4°C, lectins in the mixture formed aggregate with SGNPs, which was visually detected and easily sedimented by centrifugation. The aggregate was dissolved by adding inhibitory sugars, which were identical to the non-reducing sugar moieties on the SGNPs. According to SDS–PAGE and MS of thus obtained proteins, it was found that SGNPs isolated lectins with a high purity. For example, a protein isolated from banana using Glcα-GNP (α-glucose-immobilized gold nano-particle) was identified as banana lectin by trypsin-digested peptide-MS finger printing method.

Key words: gold nano particle, lectin, peptide MS fingerprinting, purification, sugar chain.

Abbreviations: CHCA, α-cyano-4-hydroxycinnamic acid; Glcα-GNP, alpha-glucose-immobilized gold nano-particle; GlcNAcα-GNP, alpha-*N*-acetyl-glucosamine-immobilized gold nano-particle; Manα-GNP, alpha-mannose-immobilized gold nano-particle; SA, 3,5-dimethyl-4-hydroxycinnamic acid; SGNPs, sugar-immobilized gold nano-particles.

Lectins are carbohydrate-binding proteins, which can specifically recognize sugar structures (*1*). Their physiological functions have been argued for a long time, and were recently determined for several lectins. Selectins mediate the adhesion of leucocytes and the endothelial cells of blood vessels. Some plant lectins serve as defence factors against phytopathogenic fungi, insect and animals by interacting with their glycans (*2–4*). According to these examples, lectin–glycan interactions are recognized as important in biological processes in both plant and animal bodies. To understand the functions of lectins at the molecular level in detail, purification and subsequent characterization are the most crucial.

To purify lectins from crude extract, several chromatography techniques, such as affinity chromatography, ion-exchange chromatography and gel permeation chromatography, are generally used. However, such chromatographic purification needs lengthy and tedious steps, preventing the studies of lectins especially in case of small amount of target lectins in the starting materials. To overcome this problem, a simple and effective method is desired. Use of gold nano-particles having glycans is one of the most promising for the purpose.

Gold nano-particles having glycans were rapidly developed in this decade, and utilized to analyse lectins, to estimate their affinity strength or to visualize them with electron microscopy (*5–7*). Recently, we established an efficient technique for the immobilization of glycans on gold nano-particles (*8*, *9*). The produced gold nano-particles, designated sugar-immobilized gold nano-particles (SGNPs), were homogeneous in size and amount of glycans. Importantly, they are easily sedimented by forming aggregate with lectins, suggesting that they are promising for capturing lectins. In this study, we established an effective method for purification of lectins using the SGNPs. As a result, a lectin with high purity was successfully obtained from plant extract.

MATERIALS AND METHODS

Materials—All reagents were used without further purification. Banana was obtained from a grocery store and stored at −20°C until use. Sugars were purchased as follows: maltose, cellobiose and lactose were obtained from Nacalai tesque (Kyoto, Japan); GalNAcβ1-3Gal and α1-2 mannobiose from Dextra Lab. (Reading, UK); melibiose from TCI (Tokyo, Japan). GlcNAcα1-6Glc, GlcNAcβ1-6Glc, GalNAcα1-6Glc, Fucα1-6Glc, Fucβ1-6Glc were generous gifts from Dr Wakao (Kagoshima University).

*To whom correspondence should be addressed. Tel: +81-99-285-8369, Fax: +81-99-285-8369,
E-mail: ysuda@eng.kagoshima-u.ac.jp

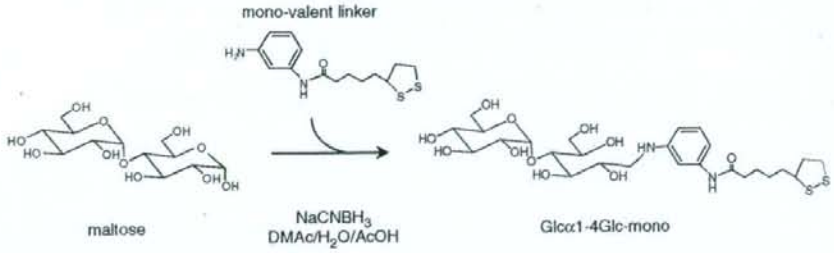

Fig. 1. Synthesis of ligand-conjugate containing α-D-glucoside (Glcα1-4Glc-mono).

Synthesis of Ligand-Conjugate Containing Sugar Moieties—Ligand-conjugates containing sugar-moieties were prepared according to the previous report (*8*, *9*). For preparation of ligand-conjugate containing α-D-glucoside (abbreviated as Glcα1-4Glc-mono), mono-valent linker compound (10.0 mg, 34 μmol) (*9*) dissolved in 1.0 ml of dimethylacetoamide (DMAc) was mixed with maltose (12.2 mg, 34 μmol, dissolved in 0.8 ml of distilled water) and 0.2 ml of acetic acid (Fig. 1). After incubation at 37°C for 4 h, $NaCNBH_3$ (21.3 mg, 340 μmol) dissolved in 0.2 ml of distilled water was added to the solution. After further incubation at 37°C for 72 h, the reaction was lyophilized. The obtained ligand-conjugate was purified by reverse-phase chromatography using Chromatorex ODS (Fuji Silysia Chemical, Aichi, Japan) equilibrated with 45% methanol at the flow rate of 0.8 ml/min. The obtained ligand conjugate was elucidated by reverse-phase chromatography using Inertsil ODS-3 (GL Science, Tokyo, Japan), MS (Voyager DE-Pro, Applied Biosystems, CA, USA) and ^1H NMR (ECA-600, JOEL, Tokyo, Japan).

By a similar protocol described above, the objected compound was prepared from appropriate materials, i.e. Glcβ1-4Glc-mono, Galα1-6Glc-mono, Galβ1-4Glc-mono, GlcNAcα1-6Glc-mono, GlcNAcβ1-6Glc-mono, GalNAcα1-6Glc-mono, GalNAcβ1-3Gal-mono, Fucα1-6Glc-mono, Fucβ1-6Glc-mono and Manα1-2Man-mono were prepared from cellobiose, melibiose, lactose, GlcNAcα1-6Glc, GlcNAcβ1-6Glc, GalNAcα1-6Glc, GalNAcβ1-3Gal, Fucα1-6Glc, Fucβ1-6Glc and α1-2 mannobiose, respectively.

Synthesis of SGNPs—Sugar-immobilized gold nanoparticles (SGNPs) were prepared according to the previous report (*8*). To synthesize α-D-glucoside immobilized SGNP (Glcα-GNP), 5 mM (final concentration) of $NaBH_4$ was added to 1 mM of aqueous solution of $NaAuCl_4$ with stirring. Above prepared 100 μM of ligand-conjugate (Glcα1-4Glc-mono) was then added to the solution with stirring. The resulting solution was subsequently dialysed against distilled water and PBST [100 mM phosphate buffer, pH 7.2, containing 0.9% (w/v) NaCl and 0.05% (v/v) Tween-20]. By TEM analysis, diameter of obtained particles was estimated to be 2–10 nm, and most of them showed around 5 nm.

Glcβ-GNP, Galα-GNP, Galβ-GNP, GlcNAcα-GNP, Glc NAcβ-GNP, GalNAcα-GNP, GalNAcβ-GNP, Fucα-GNP, Fucβ-GNP and Manα-GNP were prepared from appropriate ligand-conjugate, i.e. Glcβ1-4Glc-mono, Galα1-6Glc-mono, Galβ1-4Glc-mono, GlcNAcα1-6Glc-mono, GlcNAcβ1-6Glc-mono, GalNAcα1-6Glc-mono, GalNAcβ1-3Gal-mono, Fucα1-6Glc-mono, Fucβ1-6Glc-mono and Manα1-2Man-mono, with similar protocol. The SGNPs prepared were elucidated by binding experiment using lectins, e.g. Concanavalin A (Con A) purchased from EY Laboratories (CA, USA) and RCA120 from Vector Laboratories (CA, USA). The amount of sugar ligand attached to the gold nanoparticles was estimated by elemental analysis. As a result, 50–70 ligand-conjugates were immobilized on the surface of one gold nano-particle of 5 nm diameter.

Preparation of Plant Extract—Matured banana pulp (1 g) was homogenized in 5 ml of PBS [100 mM phosphate buffer, pH 7.2, containing 0.9% (w/v) NaCl] containing 10 mM 2-mercaptoethanol. The extract was stirred at 4°C for 2 h, and the homogenate was centrifuged at 8,000 r.p.m. for 30 min. Obtained supernatant was then filtered with DISMIC® ($\phi = 0.45$ μm, ADVANTEC, CA, USA). After adding 60% (w/v) ammonium sulphate to the filtrate, the precipitate was obtained by centrifugation at 10,000 r.p.m. for 10 min at 4°C. Thus, obtained precipitate was dissolved in 2.5 ml of PBS containing 10 mM 2-mercaptoethanol. This solution was used for the following purification steps of lectins.

Screening with SGNPs—To evaluate the sugar chain-binding properties of the extract from banana, a series of SGNPs, i.e. Glcα-GNP, Glcβ-GNP, Galα-GNP, Galβ-GNP, GlcNAcα-GNP, GlcNAcβ-GNP, GalNAcα-GNP, GalNAcβ-GNP, Fucα-GNP, Fucβ-GNP and Manα-GNP, was used for screening. In brief, the above 11 kinds of SGNP solution (30 μl, adjusted to $Abs_{530} = 3.0$) were mixed with 10 μl of sample solutions in round-bottomed microtitre plate wells, respectively, and incubated overnight at 4°C. Also, the extent of aggregation was determined by measuring the absorbance of supernatant at 530 nm. Activity was calculated according to the following equation:

$$\text{Precipitation (\%)} = 100 - \frac{Abs^{a}_{530}}{Abs^{b}_{530}} \times 100$$

where Abs^{b}_{530} and Abs^{a}_{530} indicate absorbance at 530 nm before and after overnight incubation, respectively.

Dissociation of SGNP–Lectin Complex with Free Sugars—Dissociation effects of free sugars against SGNP aggregates were examined. Similar to the screening described above, 30 μl of Glcα-GNP was mixed with

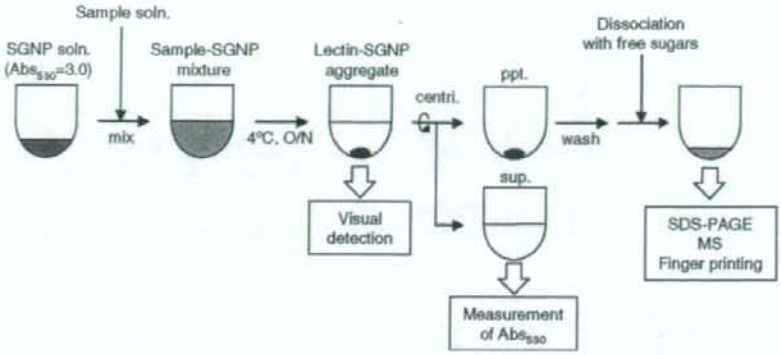

Scheme 1. **The procedure for capturing lectins using SGNPs.** Several SGNPs, e.g. Manα-GNP, Glcα-GNP and Galβ-GNP, can be used. After subsequent washing with appropriate buffer and distilled water, aggregate was dissolved in inhibitory sugar solutions and applied to subsequent analyses.

10 μl of sample solution. After standing at room temperature for 10 min, the formed SGNP aggregate was sedimented by centrifugation at 1,800 r.p.m. for 1 min at room temperature. After removal of supernatant, 100 μl of sugar solutions (0.2 M glucose, GlcNAc, mannose and galactose dissolved in distilled water) were added to each well.

Capturing Lectins—Sugar-binding proteins (lectins) were captured by SGNPs and characterized. The overall approach was shown in Scheme 1. From data of screening, 30 μl of Glcα-GNP, GlcNAcα-GNP or Manα-GNP was added to 10 μl of banana extract, and thoroughly mixed by pipetting. After incubation overnight at 4°C, the formed aggregate was sedimented by centrifugation at 10,500 r.p.m. for 10 min, and the supernatant was removed. After subsequent washing with 50 μl each of PBST and distilled water, the aggregate was dissolved by adding 10 μl of inhibitory monosaccharides, *i.e.* 0.2 M glucose, 0.2 M GlcNAc and 0.2 M mannose were used for Glcα-GNP, GlcNAcα-GNP and Manα-GNP, respectively. Thus, captured proteins were analysed by SDS–PAGE under non-reducing condition using 15% gel without further purification. Also, they were applied to the subsequent analyses described below.

Proteolytic Digestion by Trypsin—After re-dissolving in inhibitory sugar solutions, 10 μl aliquot of sample solution (corresponding to 2.3 μg protein) was added to the same volume of 75 mM NH_4HCO_3. Proteins in the solution were denatured by boiling for 5 min, and then 10 μl of trypsin (Sigma–Aldrich, MO, USA) dissolved in distilled water (5 μg/ml) was added. The protein digestion was performed by incubating the reaction solution at 37°C for 2 h. The resulting digest was analysed by MALDI-TOF/MS without further purification.

MALDI-TOF Mass Spectrometry—The MALDI-TOF mass spectrometer used was a Voyager DE-Pro (Applied Biosystems). α-cyano-4-hydroxycinnamic acid (CHCA) or 3,5-dimethyl-4-hydroxycinnamic acid (SA) as MALDI matrix was dissolved in the aqueous solution containing 50% acetonitrile and 0.1% trifluoroacetic acid (TFA) to make 10 mg/ml. SGNP-captured proteins and the trypsin-digested peptides were co-crystallized with CHCA or SA matrix. The MS analyses were performed with a reflector and positive-ion mode. The spectra were acquired with 300 shots of a 337 nm nitrogen laser operating at 3 Hz. Angiotensin (SIGMA) and Calibration mixture 2 (PE Biosystems, CA, USA) were used as MS calibration standards. Protein identification was performed by searching the National Center for Biotechnology Information (NCBI) non-redundant database using Mascot search engine (http://www.matrixscience.com/search_form_select.html). The following parameters were used for database searches with MALDI-TOF peptide mass fingerprinting: monoisotopic mass, ±1.2 Da peptide mass tolerance, trypsin as digestion enzyme with one missed cleavage allowed, no modification of a cysteine residue.

RESULTS AND DISCUSSION

To purify lectins from biological materials, the most efficient way may be to utilize their affinity for sugar chains. Since lectins specifically recognize sugar structures, it is essential to select appropriate sugar chains. Thus, we first screened the sugar-binding property of the extract using a series of SGNPs, i.e. Glcα-GNP, Glcβ-GNP, Galα-GNP, Galβ-GNP, GlcNAcα-GNP, GlcNAcβ-GNP, GalNAcα-GNP, GalNAcβ-GNP, Fucα-GNP, Fucβ-GNP and Manα-GNP. The banana extract was thoroughly mixed with 11 kinds of SGNPs and allowed to stand at 4°C. When banana extract includes agglutinin having affinity for particular SGNPs, lectin-SGNP aggregate may be formed, and it is visually detected as precipitate. As a result, three of the SGNPs tested, i.e. Glcα-GNP, GlcNAcα-GNP and Manα-GNP, obviously formed precipitate (Fig. 2). In contrast, no precipitate was detected for the other SGNPs including Glcβ-GNP and GlcNAcβ-GNP. To know the extent of aggregation, the absorbance of supernatant at 530 nm was measured. As shown in Fig. 2, 91.2%, 92.4% and 92.8% of Glcα-GNP, GlcNAcα-GNP and Manα-GNP, respectively, in the wells precipitated, while the β-anomers showed no or, if any, weak affinity for banana extract. These results clearly

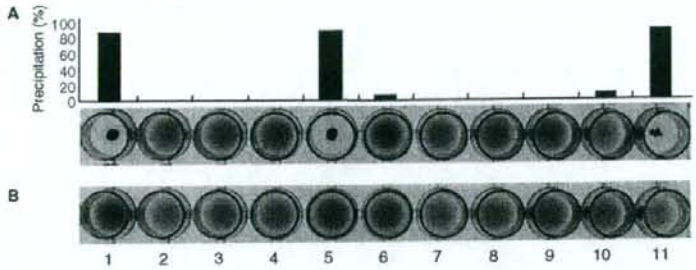

Fig. 2. **Screening of sugar-immobilized gold nano-particles (SGNPs).** Ten microlitres of sample solutions were added to 30 µl of each SGNP in round-bottomed microtitre plate wells. When the sample solution includes lectin(s) having affinity for particular SGNP(s), lectin–SGNP aggregate is formed and observed as a precipitate. Graphs indicate the extent of aggregation determined by measuring the absorbance of supernatant at 530 nm. (A) Banana extract, (B) PBST as negative control. 1: Glcα-GNP, 2: Glcβ-GNP, 3: Galα-GNP, 4: Galβ-GNP, 5: GlcNAcα-GNP, 6: GlcNAcβ-GNP, 7: GalNAcα-GNP, 8: GalNAcβ-GNP, 9: Fucα-GNP, 10: Fucβ-GNP, 11: Manα-GNP.

indicated that banana extract included agglutinin having affinity for α-glucose, α-GlcNAc and α-mannose. The sugar-binding specificity observed here agrees well with previous reports describing that lectin in banana pulp shows affinity for mannose, glucose, GlcNAc and their derivatives (*10–13*).

To clarify sugar-binding specificity in detail, dissociation effects of free sugars were examined using Glcα-GNP. Similar to the case of screening described above, 30 µl of Glcα-GNP was mixed with 10 µl of banana extract. After standing at room temperature for 10 min, aggregate was sedimented by centrifugation at 1,800 r.p.m. for 1 min, and supernatant was removed. To the wells, 100 µl of sugar solutions, i.e. 0.2 M glucose, 0.2 M GlcNAc, 0.2 M mannose or 0.2 M galactose dissolved in distilled water, was added, respectively. As expected, Glcα-GNP-aggregate was re-dissolved in glucose solution (Fig. 3). In addition, it was also re-dissolved in GlcNAc and mannose solution, but not at all in galactose solution (Fig. 3). The result indicated that the banana extract included an agglutinin having affinity for glucose, mannose and GlcNAc. In other words, the protein aggregated with Glcα-GNP, GlcNAcα-GNP or Manα-GNP may be identical.

Using Glcα-GNP, GlcNAcα-GNP or Manα-GNP, the purification of the agglutinin from banana extract was performed. As shown in Scheme 1, 10 µl of banana extract was added to 30 µl of each SGNP. The formed aggregates were sedimented by centrifugation, and supernatant was transferred to other tubes. Precipitates were subsequently washed with PBS containing 0.05% Tween-20 (PBST) and distilled water to remove non-specifically bound proteins and salt, and then re-dissolved in inhibitory sugar solutions. As estimated by quantifying the protein using a dye-binding assay (*14*), 2.3, 4.3 and 3.6 µg proteins were captured from 10 µl of extract (corresponding to 4 mg starting plant material) using Glcα-GNP, GlcNAcα-GNP and Manα-GNP, respectively. Higher yield relative to previous report (*11*) was probably achieved by one-tube reaction. Upon SDS–PAGE under non-reducing conditions, every SGNP-captured protein showed a single protein band at a molecular mass 13.6 kDa (Fig. 4, lanes 4, 6 and 8). No band was detected at the corresponding mass in

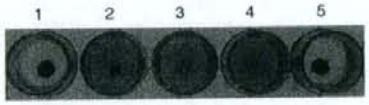

Fig. 3. **Dissociation of SGNP–lectin complex with free sugars.** Lectin–Glcα-GNP aggregate is first formed. After removal of supernatant, sugar solutions were added to each well. When lectin–SGNP interaction is inhibited by free sugars added, lectin will dissociate from the SGNP and the aggregate disappears. (1) PBS, (2) glucose, (3) GlcNAc, (4) mannose, (5) galactose.

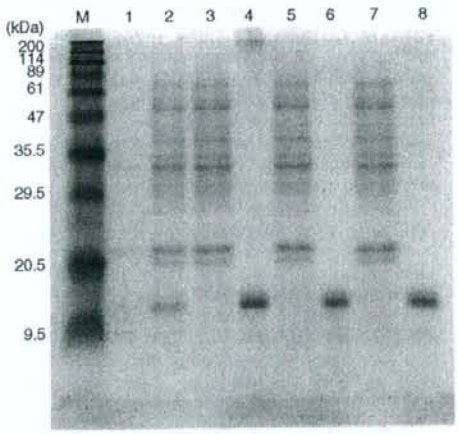

Fig. 4. **SDS–PAGE of proteins obtained from banana stained with CBB.** M: Molecular marker, lane 1: crude extract from plant materials, lane 2: extract after concentration with 60% (w/v) ammonium sulphate, lanes 3 and 4: Glcα-GNP, lanes 5 and 6: GlcNAcα-GNP, lanes 7 and 8: Manα-GNP. Lanes 3, 5 and 7: supernatant after aggregation, lanes 4, 6 and 8: precipitation after aggregation.

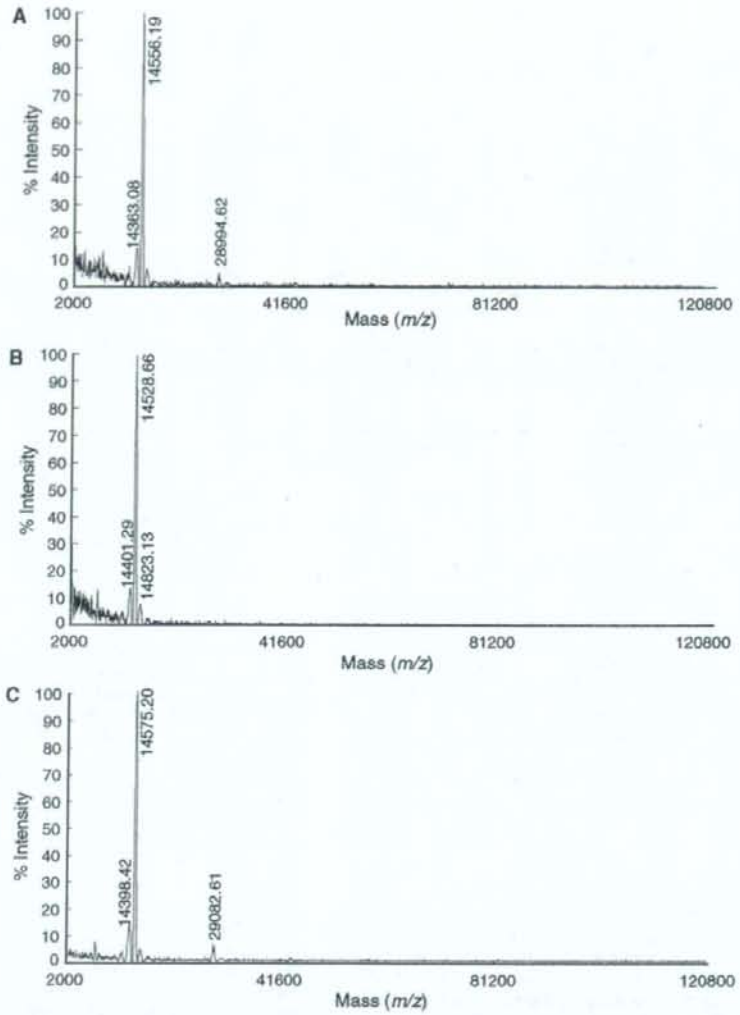

Fig. 5. **MALDI-TOF mass spectra of proteins obtained from banana extract using Glcα-GNP (A), GlcNAcα-GNP (B) and Manα-GNP (C).**

supernatant (Fig. 4, lanes 3, 5 and 7). This result indicated that the protein with molecular mass 13.6 kDa in the extract was completely captured by SGNPs. Also, the captured proteins are very pure, as far as stained with CBB.

Exact molecular mass of captured proteins was then measured By MALDI-TOF MS analysis. Since aggregates were washed with distilled water and dissolved in sugar solutions without salts, SGNP-captured proteins were used for MS analysis without further purification and desalting steps. For analysis, 1.2, 2.2 and 1.8 μg of Glcα-GNP-, GlcNAcα-GNP- and Manα-GNP-captured proteins (corresponding to 5 μl of extract, *i.e.* 2 mg of starting plant material), respectively, was co-crystallized with SA, and directly analysed by MALDI-TOF mass spectrometer. As a result, intense signals were detected for all the three samples (Fig. 5), in spite of remaining free SGNPs. The result indicates that free SGNPs did not disturb the ionization of proteins in MALDI-TOF/MS, suggesting that the SGNP was not needed to be removed from the analytical samples. In case of Glcα-GNP-captured protein, only one major peak was detected at m/z value of 14,556 (Fig. 5A). According to the previous report, mannose/glucose-binding lectin from banana pulp

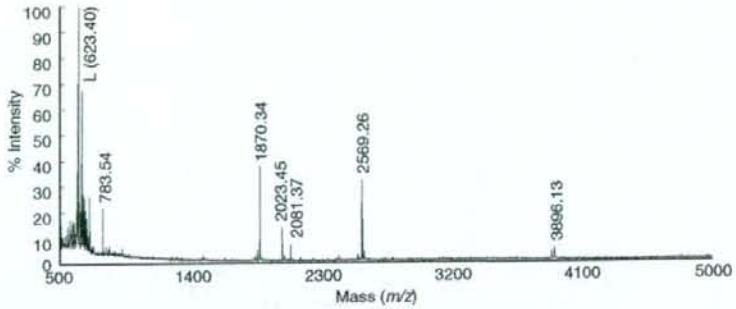

Fig. 6. **MALDI-TOF mass spectra from tryptic digestion of proteins obtained from banana extract using Glcα-GNP.** All the six peaks submitted to the Mascot search engine for database searching was matched for total sequence coverage of 76%. L denotes m/z value of ligand conjugate.

Table 1. **Peptide peaks detected from the tryptic digestion of Glcα-GNP-captured proteins.**

	m/z	Protein	Start–End	Missed cleavage	Sequence
1	1870.40	Banana lectin	7–25	0	VGAWGGNGGSAFDMGPAYR
2	2081.37	Banana lectin	31–49	0	IFSGDVVDGVDVTFTYYGK
3	2569.26	Banana lectin	31–53	1	IFSGDVVDGVDVTFTYYGKTETR
4	3896.13	Banana lectin	54–91	0	HYGGSGGTPHEIVLQEGEYLVGMAGEVANYHGAVVLGK
5	2023.45	Banana lectin	100–120	0	AYGPFGNTGGTPFSLPIAAGK
6	783.55	Banana lectin	121–127	0	ISGFFGR

is a dimeric protein composed of 15 kDa subunits estimated by SDS–PAGE (*10*, *11*). In addition, its molecular weight calculated from sequence (Accession No: 2BMYA) is 14,554 Da (*15*). Thus, the captured protein is supposed to be a banana lectin. Since gene of banana lectin is a member of a multi-gene family (*11*), a weak signal at m/z value of 14,363 might be derived from them. Another minor signal at m/z value of 28,994 was corresponding to a dimer of banana lectin. Very similar MS profiles were observed for GlcNAcα-GNP and Manα-GNP (Fig. 5B and C). In both cases, only one major peak was detected around m/z = 14,550. The m/z value of major peaks observed for GlcNAcα-GNP and Manα-GNP were 14,528 and 14,575, respectively, which are corresponding to the previous report, too (*11*). According to the results of MS analysis together with those of SDS–PAGE, the purity of captured proteins was high enough to apply further analysis.

To identify SGNP-captured protein, we carried out peptide-mass fingerprinting. Judging from the results of dissociation of SGNP–lectin complex with free sugars, SDS–PAGE and MS spectrometry described above (Figs 3, 4 and 5), all the proteins captured by Glcα-GNP, GlcNAcα-GNP and Manα-GNP were supposed to be identical. Thus, Glcα-GNP-captured protein was used for the purpose. As described under MATERIALS AND METHODS section, the captured protein (2.3 μg protein) was digested by trypsin, and the resulting digests were analysed by the MALDI-TOF/MS (Fig. 6). Detected peaks at m/z 783.54, 1870.34, 2023.45, 2081.37, 2569.26 and 3896.13 were searched against the Swiss-Prot protein database for the identification of source proteins. All six peaks matched the database. The peptide sequences from the digested protein are listed in Table 1. As expected, all the peaks are revealed to be derived from banana lectin. The sequence coverage was 76%. Thus, Glcα-GNP-captured protein was identified as banana lectin. This result indicated that the purity of protein captured by Glcα-GNP was sufficient to identify the source protein.

In conclusion, we established an effective method for a one-step purification of lectin from extracts using SGNPs. Compared with conventional methods, several advantages of SGNPs were found, e.g. small amount of start materials (in case of banana lectin, <1 g), simple operation (only centrifugation) and direct analysis by SDS–PAGE and MS spectrometry (without further purification or concentration steps). Although SGNPs having simple saccharides were used here, a lectin was successfully purified with such high purity as to identify the source protein. Using a similar protocol, we have also performed easy and quick purification of lectins from soybean. Since, in general, affinities of lectins for oligosaccharides are relatively high compared with those for simple saccharides, utilization of SGNPs having complex glycans is promising for easy purification of less abundant carbohydrate-binding proteins.

We thank Y. Fujimoto, Osaka University, for her help in elemental analysis. This research was supported in part by a grant from a Ministry of Health, Labor and Welfare (Y.S.), and Japan Science and Technological Agency (CREST, Y.S.).

REFERENCES

1. Sharon, N. and Lis, H. (2003) *Lectins*. 2nd edn, pp. 1–4 Kluwer Academic Publishers, Boston

2. Kijune, J.W. (1996) Function of plant lectins. *Chemtracts – Biochem. Mol. Biol.* **6**, 180–187
3. Van Damme, E.J.M., Peumans, W.J., Pusztai, A., and Bardocz, S. (1998) *Handbook of Plant Lectins: Properties and Biomedical Applications*. p. 452 John Wiley and Sons, Chichester
4. Murdock, L.L. and Shade, R.E. (2002) Lectins and protease inhibitors as plant defenses against insects. *J. Agric. Food. Chem.* **50**, 6605–6611
5. Otsuka, H., Akiyama, Y., Nagasaki, Y., and Kataoka, K. (2001) Quantitative and reversible lectin-induced association of gold nanoparticles modified with alpha-lactosyl-omega-mercapto-poly(ethylene glycol). *J. Am. Chem. Soc.* **123**, 8226–8230
6. Hone, D.C., Haines, A.H., and Russell, D.A. (2003) Rapid, quantitative calorimetris detection of a lectin using mannose-stabilized gold nanoparticles. *Langmuir* **19**, 7141–7144
7. Lin, C.C., Ye, Y.C., Yang, C.Y., Chen, C.L., Chen, G.F., Chen, C.C., and Wu, Y.C. (2002) Selective binding of mannose-encapsulated gold nanoparticles to type 1 pili in Escherichia coli. *J. Am. Chem. Soc.* **124**, 3508–3509
8. Suda, Y., Kishimoto, Y., Nishimura, T., Yamashita, S., Hamamatsu, M., Saito, A., Sato, M., and Wakao, M. (2006) Sugar-immobilized gold nano-particles (SGNP): novel bioprobe for the on-site analysis of the oligosaccharide protein interactions. *Polymer Preprints* **47**, 156–157
9. Suda, Y., Arano, A., Fukui, Y., Koshida, S., Wakao, M., Nishimura, T., Kusumoto, S., and Sobel, M. (2006) Immobilization and clustering of structurally defined oligosaccharides for sugar chips: an improved method for surface plasmon resonance analysis of protein carbohydrate interactions. *Bioconjug. Chem.* **17**, 1125–1135
10. Koshte, V.L., van Dijk, W., van der Stelt, M.E., and Aalberse, R.C. (1990) Isolation and characterization of BanLec-I, a mannoside-binding lectin from *Musa paradisiac* (banana). *Biochem. J.* **272**, 721–726
11. Peumans, W.J., Zhang, W., Barre, A., Houles Astoul, C., Balint-Kurti, P.J., Rovira, P., Rouge, P., May, G.D., Van Leuven, F., Truffa-Bachi, P., and Van Damme, E.J.M. (2000) Fruit-specific lectins from banana and plantain. *Planta* **211**, 546–554
12. Mo, H., Winter, H.C., Van Damme, E.J., Peumans, W.J., Misaki, A., and Goldstein, I.J. (2001) Carbohydrate binding properties of banana (*Musa acuminata*) lectin I. Novel recognition of internal alpha1,3-linked glucosyl residues. *Eur. J. Biochem.* **268**, 2609–2615
13. Winter, H.C., Oscarson, S., Slattegard, R., Tian, M., and Goldstein, I.J. (2005) Banana lectin is unique in its recognition of the reducing unit of 3-O-beta-glucosyl/mannosyl disaccharides: a calorimetric study. *Glycobiology* **15**, 1043–1050
14. Bradford, M. (1976) A rapid and sensitive method for the quantitation of microgram quantities of protein utilizing the principle of protein-dye binding. *Anal. Biochem.* **72**, 248–254
15. Meagher, J.L., Winter, H.C., Ezell, P., Goldstein, I.J., and Stuckey, J.A. (2005) Crystal structure of banana lectin reveals a novel second sugar binding site. *Glycobiology* **15**, 1033–1042